COMPONENT PART NOTICE

THIS PAPER IS A COMPONENT PART OF THE FOLLOWING COMPILATION REPORT:

TITLE: Minutes of the Explosives Safety Seminar (22nd) Held in Anaheim, California on 26-28 August 1986. Volume 2.

TO ORDER THE COMPLETE COMPILATION REPORT, USE AD-A181 275.

THE COMPONENT PART IS PROVIDED HERE TO ALLOW USERS ACCESS TO INDIVIDUALLY AUTHORED SECTIONS OF PROCEEDING, ANNALS, SYMPOSIA, ETC. HOWEVER, THE COMPONENT SHOULD BE CONSIDERED WITHIN THE CONTEXT OF THE OVERALL COMPILATION REPORT AND NOT AS A STAND-ALONE TECHNICAL REPORT.

THE FOLLOWING COMPONENT PART NUMBERS COMPRISE THE COMPILATION REPORT:

AD#: P005 350 thru P005 393 AD#:

AD#: AD#:

AD#: AD#:

Accession For	
NTIS GRA&I	X
DTIC TAB	☐
Unannounced	☐
Justification	
By	
Distribution/	
Availability Codes	
Dist	Avail and/or Special
A-1	

BLAST LOADING ON ABOVE GROUND BARRICADED MUNITION STORAGE MAGAZINES - II

by
George A. Coulter
Charles N. Kingery
Peter C. Muller

U.S. Army Materiel Command
Ballistic Research Laboratory
Aberdeen Proving Ground, Maryland 21005-5066

ABSTRACT

This report presents the results of a study designed to measure the blast loading on above ground munition storage magazines. The magazines are sited at separation distances of K2 ($2W^{1/3}$ ft), K4 ($4W^{1/3}$ ft), and K6 ($6W^{1/3}$ ft) where W is the maximum allowable high-explosive weight in pounds mass. Earth barricades protect the structures. Responding and nonresponding 1/23.5 scaled models were used for the test program. Loading results are presented for the nonresponding barricaded model magazine. The highest loading measured on the nonresponding model was on the side-wall nearest the donor magazine. Maximum values of reflected pressure at Station 3 were found to be about 900, 600, and 360 kPa for separation distances of $0.8\ Q^{1/3}$ m, $1.6\ Q^{1/3}$ m, and $2.4\ Q^{1/3}$ m, respectively. Whole wall translation velocities calculated from the measured wall loading forces ranged from 7-12 m/s. These velocities are well under the fragment velocities needed to cause detonation of the stored munitions in the acceptor magazine. This indicated the present siting criteria of $0.8\ Q^{1/3}$ m is safe for this type of above ground barricaded magazine. Additional costly greater siting distances should not be necessary.

I. INTRODUCTION

A. Background

This study is a portion of a research program conducted at the Ballistic Research Laboratory (BRL) and sponsored by the Department of Defense Explosives Safety Board (DDESB). The purpose of the general program is to model and measure blast parameters pertaining to various types of munition storage magazines. This study concerns an above ground type barricaded storage magazine, but without earth cover. This type of magazine has been located in areas of Europe and in the United Kingdom. The particular one selected for study is located in Machrihanish,Scotland, Reference 1. Preliminary research at BRL was reported in Reference 2.

B. Objective

The primary objective of this phase of the research is to determine through scale model experiments the blast loading on an acceptor magazine with differing barricades in the event of an accidental explosion in a donor magazine. An assumption is made that all the stored munition (net explosive weight, NEW) in the donor magazine detonates together to create the blast wave. Effects of the munitions casing are not considered, although, for the particular contents of a known storage magazine it could be included.

All barricades were constructed of hard packed soil. Results from Reference 2 indicated a need to control this parameter. Safe separation distances of $0.8\ Q^{1/3}$ m, $1.6\ Q^{1/3}$ m, and $2.4\ Q^{1/3}$ m, where Q is in kilograms, were to be modeled with the experiments. These distances correspond to K2 ($2W^{1/3}$ ft), K4 ($4W^{1/3}$ ft) and K6 ($6W^{1/3}$ ft) where w is in pounds mass.

II. TEST PROCEDURES

The types of models, test site layout, instrumentation,and test matrix will be discussed in this section.

A. Models

Two types of scaled models were used for the test program. A steel nonresponding acceptor model was built and instrumented with piezoelectric pressure transducers. The second model was a scaled concrete model (density was same as full-size magazine) used both for the donor and the responding acceptor (Shot 1 only).

Figure 1 shows photographs and a sketch of the 1/23.5 scale nonresponding steel model of a munitions magazine located at the Machrihanish, Scotland site. The assumption is made that the variety of stored munitions in the full-sized magazine will be equivalent to 13,000 kg of bare hemispherical Pentolite. This amount is scaled down by the cube root or to 1/23.5 scale for the 1 kg charge that was used for these tests. The model dimensions and transducer locations are shown in Figure 1-C.

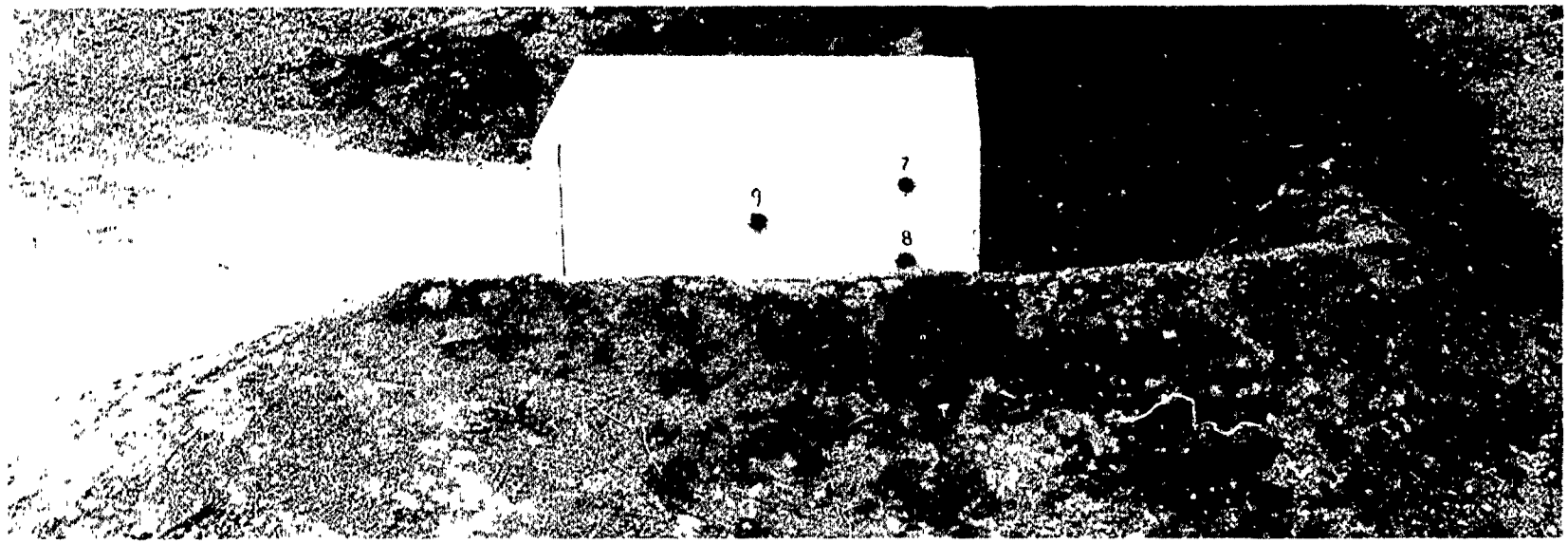

A. View of Back Side Wall

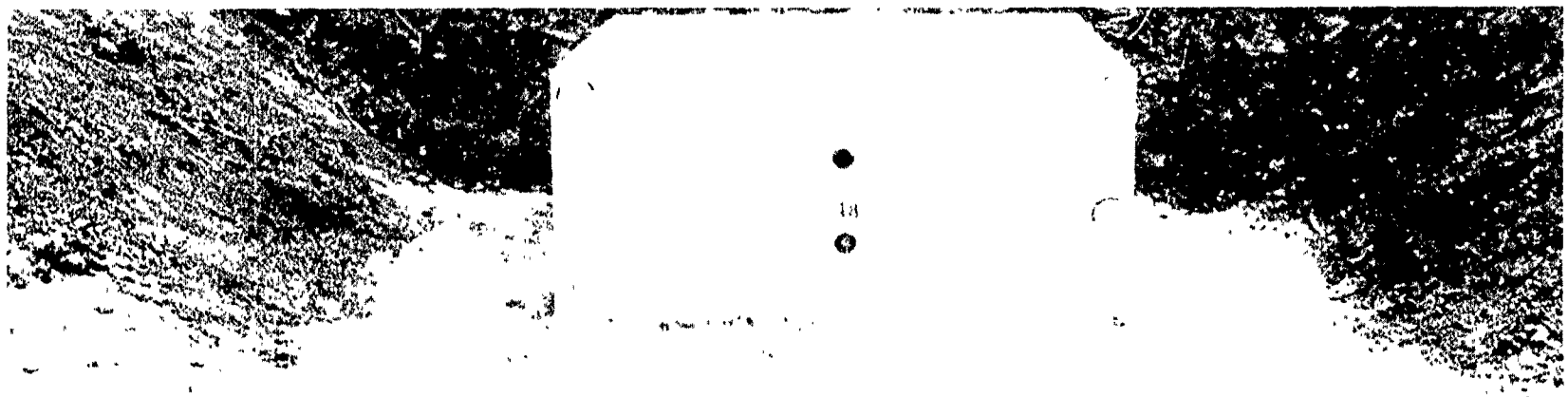

B. View of Right End Wall

Figure 1. Nonresponding Acceptor Model

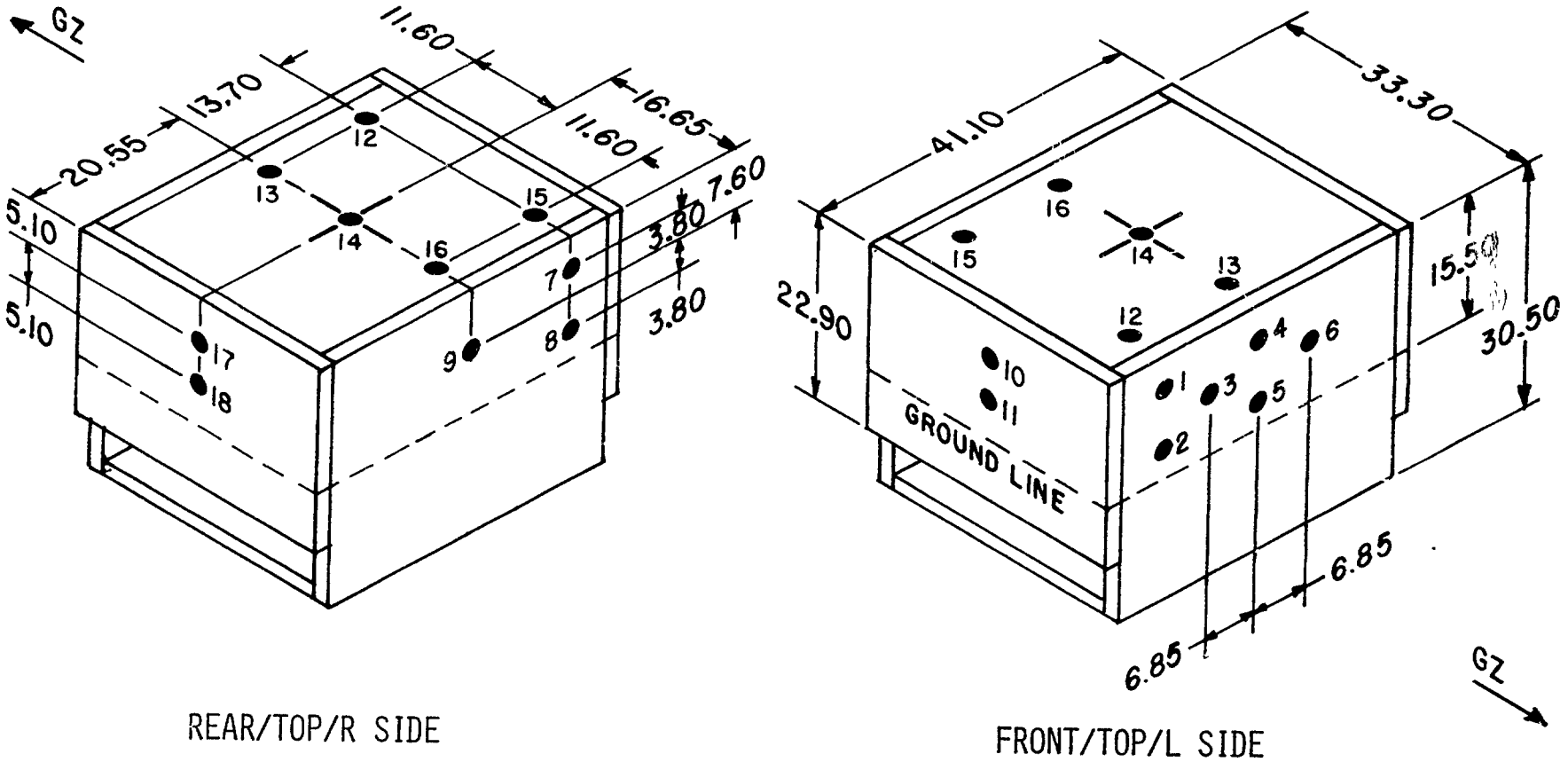

C. Sketch Showing Station Locations

Figure 1. Nonresponding Acceptor Model (Cont.)

The near side-wall is defined as the wall closest to the magazine. All positions are defined as seen from the donor magazine.

The concrete donor/acceptor model was also 1/23.5 scale; it is shown in the photographs of Figures 2 and 3. The concrete models were cast as five separate slabs. The door opening was closed during the shot by a cardboard door. A ready-mixed mortar cement was used for the roof and wall portions. Copper wire was used as reinforcing for the roof slab only.

For Shot 1, the responding acceptor model had the near side-wall scored to control the break-up mode. Additionally, the model slabs were cemented at the joints with silastic cement to insure that the side wall would fail first as would be expected for the full-size magazine.

A styrofoam witness plate was placed against the back wall to catch any flying fragments. A simple indication of the break-up pattern might be obtained in this manner. A more sophisticated velocity screen system is planned for use during future tests.

B. Test Charges

The bare charges were cast in-house with a 50/50 mix Pentolite in a hemispherical mold. All charges were trimmed to be exactly 1 kg. Detonation was from the center of the flat surface of the charge placed on the donor's floor.

C. Test Layout

Figures 4-6 show sketches of the test site layout. All dimensions, including barricades, were scaled by the 1/23.5 factor chosen for the model and the charge. It was decided at a meeting with the DDESB Project Officer not to change the spacing between the models and the back barricade. Spacing was changed between the model magazines according to multiples of the safe separations distances: $0.8\ Q^{1/3}$ m, $1.6\ Q^{1/3}$ m, and $2.4\ Q^{1/3}$ m.

D. Instrumentation

The instrumentation was standard for blast wave recording. The transducers were quartz PCB piezoelectric type, Models 113A24 and 113A28. These were coupled through preamplifiers into either a Honeywell 7600 or 101 FM recording system. The data were available from a visicorder immediately after the shot. Later the data were reduced to plots with engineering units for comparison. An analog-digital system coupled to a microcomputer accomplished this phase of the data reduction. See Figure 7 for a schematic.

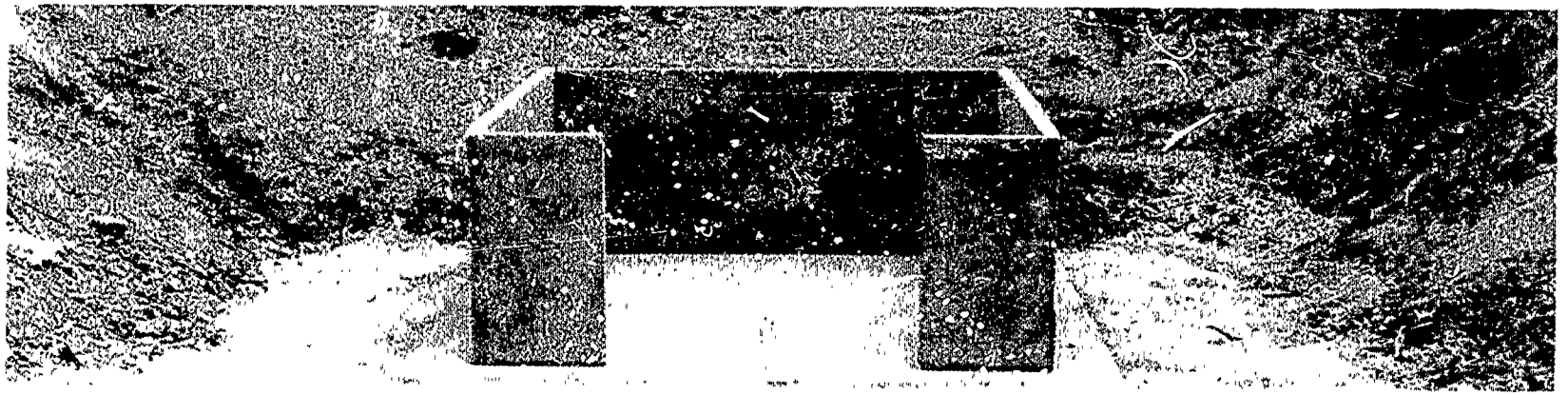

A. Donor without Roof Slab

B. Acceptor

Figure 2. Concrete Donor/Acceptor Models

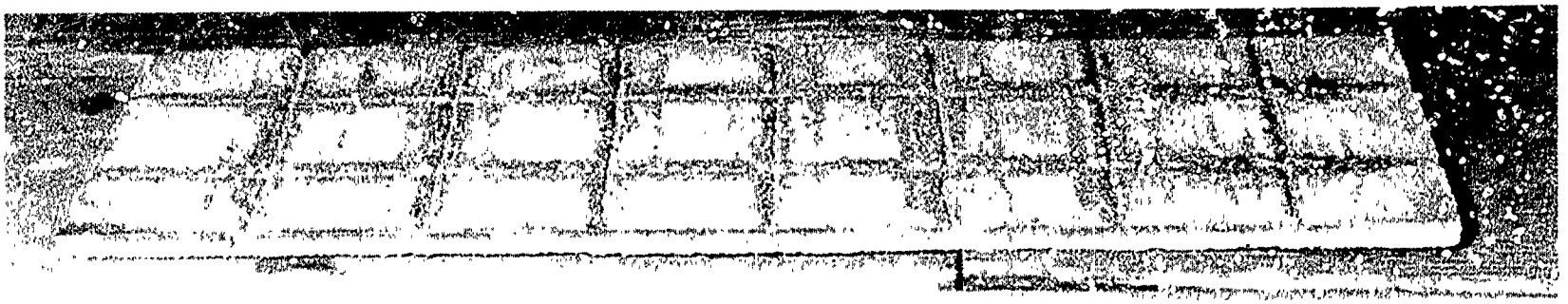

A. Scored Near Side-Wall

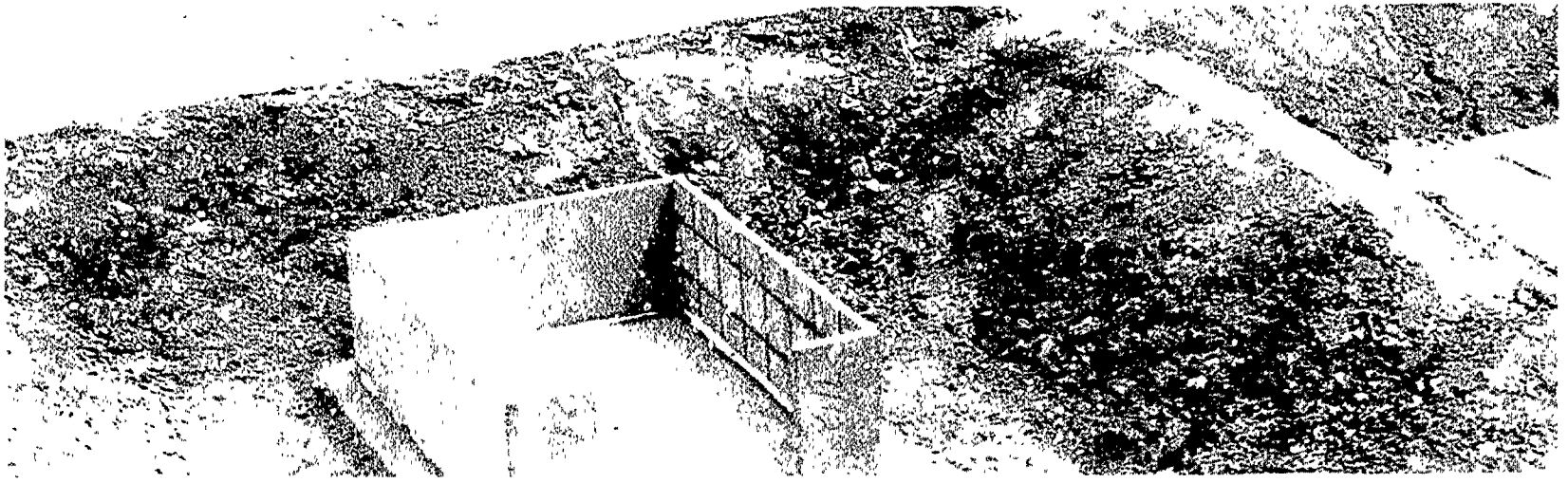

B. Installed Wall

Figure 3. Concrete Responding Acceptor Model

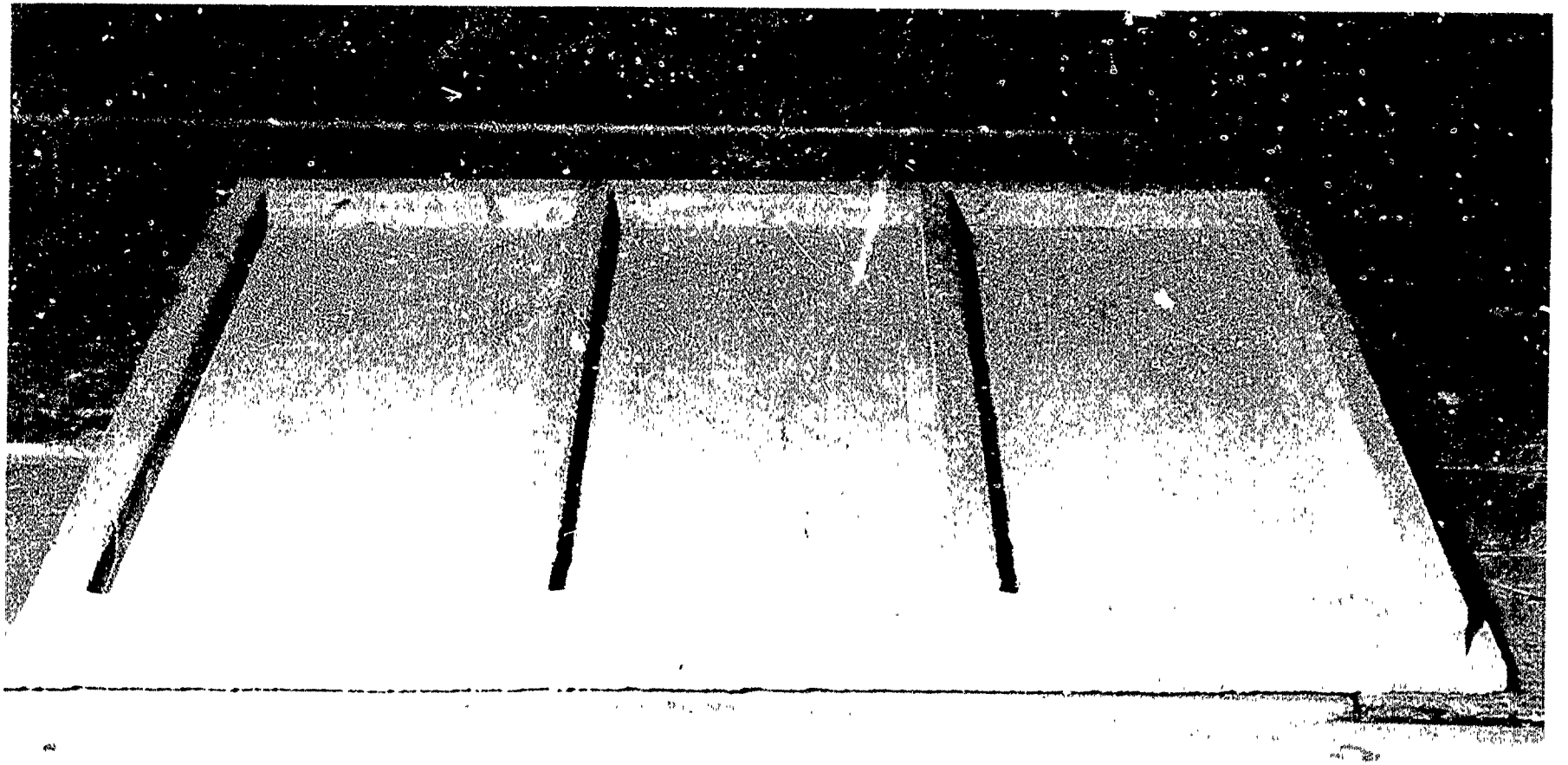

C. Reinforced Donor/Acceptor Roof

Figure 3. Concrete Responding Acceptor Model (Cont.)

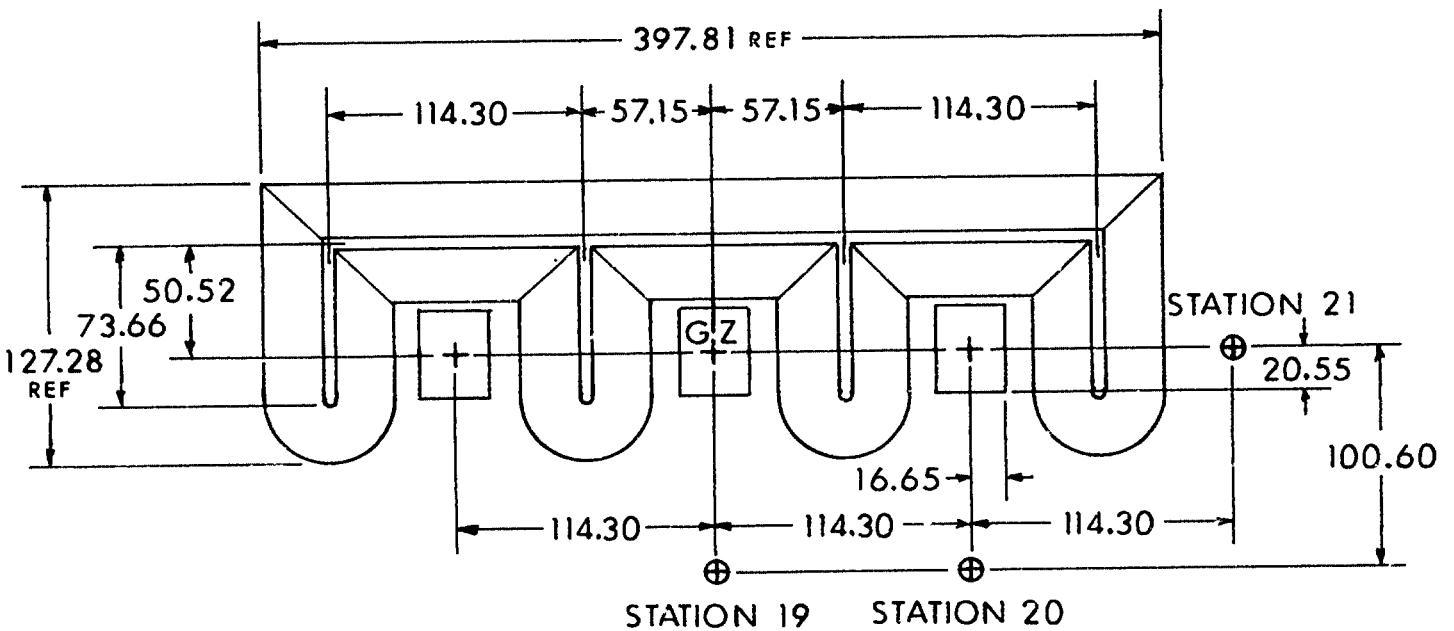

DIMENSIONS IN CENTIMETRES

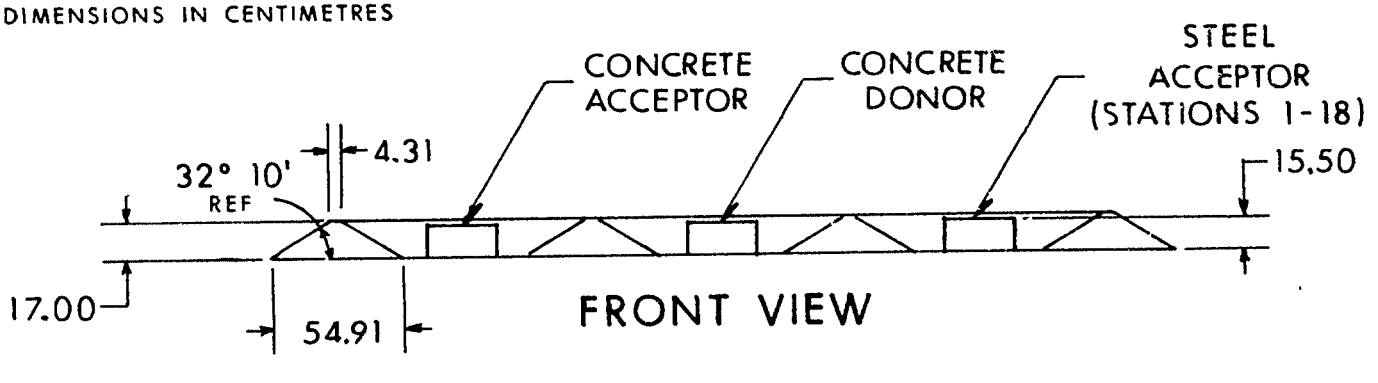

Figure 4. Test layout for a Separation Distance of 0.8 $Q^{1/3}$ m

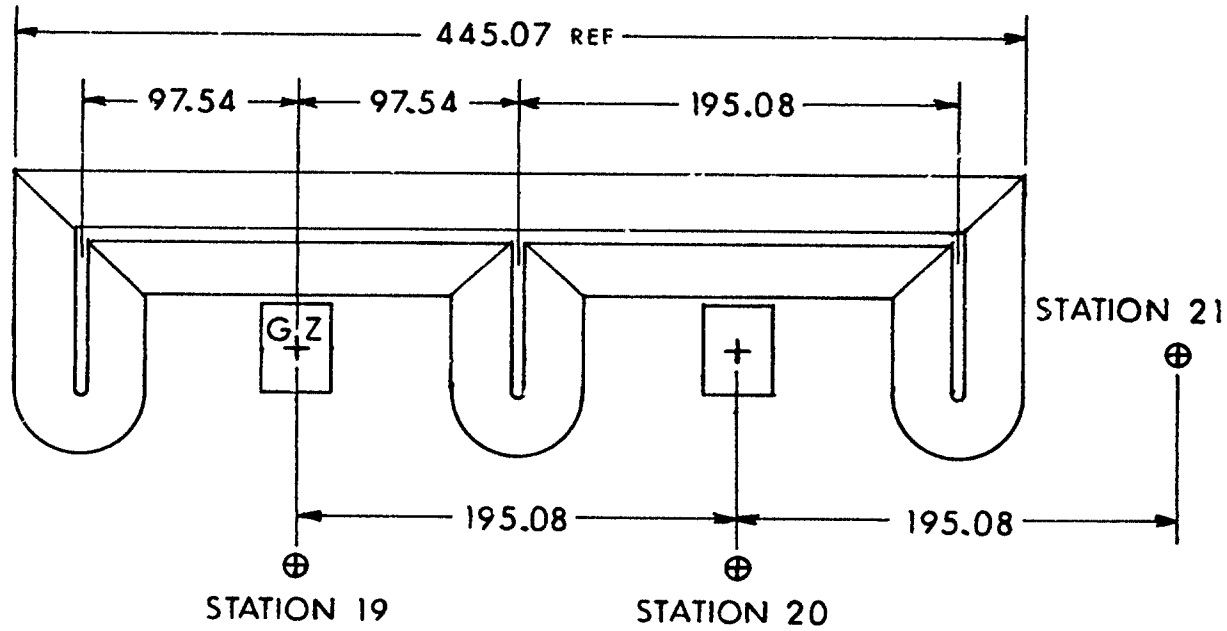

Figure 5. Test Layout for a Separation Distance of 1.6 $Q^{1/3}$ m

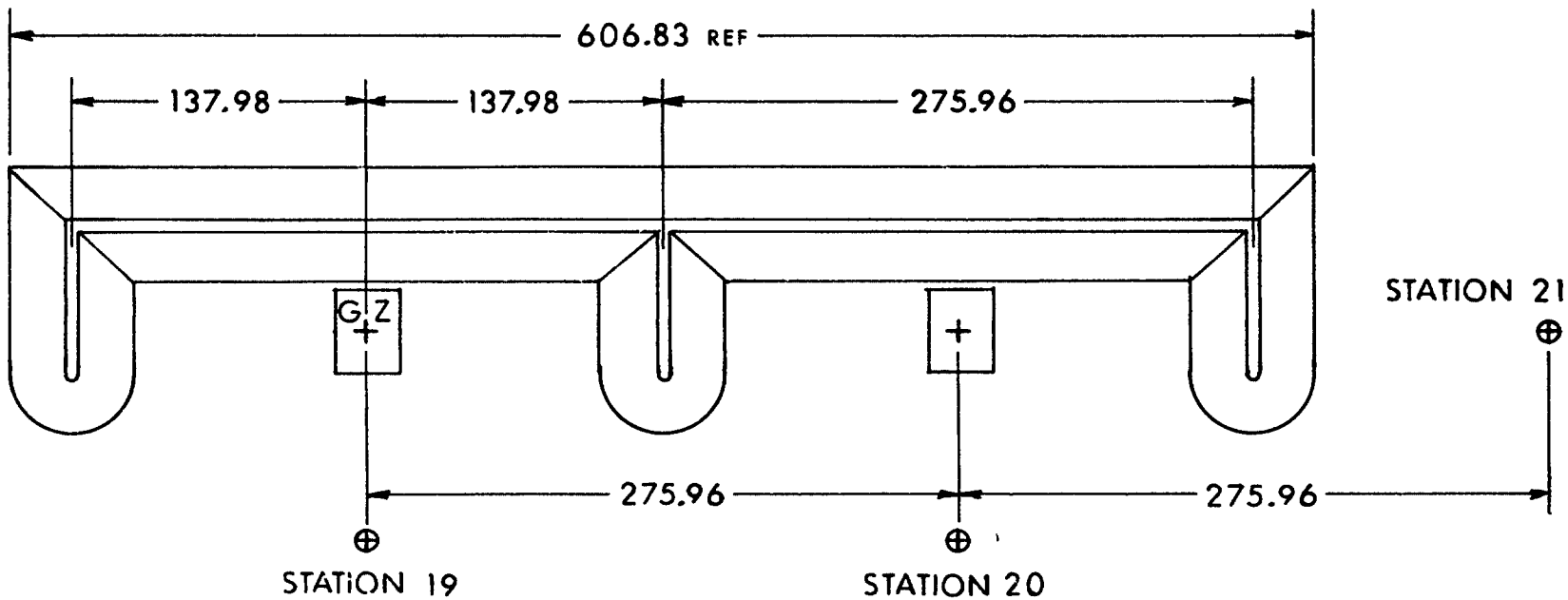

Figure 6. Test Layout for a Separation Distance of 2.4 $Q^{1/3}$ m

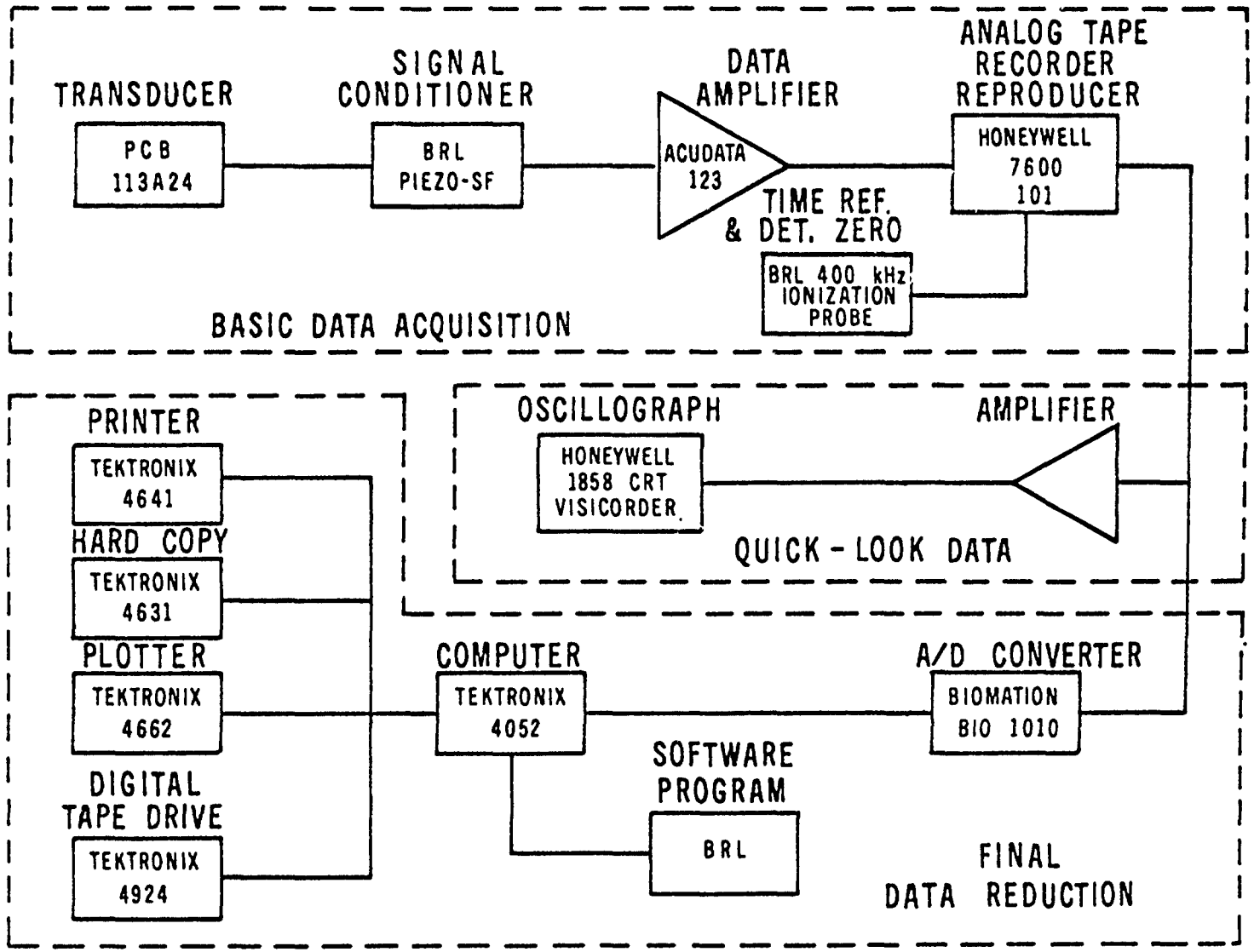

Figure 7. Data Acquisition/Reduction System

E. Test Matrix

A series of six shots was fired during the test period. For the test conditions at the Range 8 test site on Spesutie Island, see Table 1. A responding concrete acceptor model was used only on Shot 1. The remaining shots were made only with the non-responding instrumented steel acceptor. All Pentolite charges were cast and trimmed to be 1 kg hemispherical to make the test comparisons more exact. No scaling was needed between shots. All barricades were constructed of field soil, hard-packed.

TABLE 1. TEST MATRIX

Shot	Donor Cover kg	50/50 Pentolite Charge Weight kg	Concrete Acceptor	Ambient Pressure kPa	Ambient Temp. °C	Wind Speed km/h	Separation Distance Factor
1	5.72	1.00	Yes	101.5	30.0	12 @ 280°	K2
2	5.71	1.00	No	101.9	28.3	5 @ 190°	K4
3	5.33	1.00	No	102.9	25.0	3 @ 90°	K4
4	5.64	1.00	No	102.2	26.1	5 @ 90°	K6
5	5.50	1.00	No	101.8	30.3	5 @ 80°	K6
6	5.50	1.00	No	100.6	29.4	Calm	K6

	English	Metric
Note:	$K2 = 2W^{1/3}$ ft	$= 0.8Q^{1/3}$ m
	$K4 = 4W^{1/3}$ ft	$= 1.6Q^{1/3}$ m
	$K6 = 6W^{1/3}$ ft	$= 2.4Q^{1/3}$ m

for K2 English: W = 2.204 lbs, the K2 = 2(1.30)ft = 2.60 ft.

for K2 metric: Q = 1 kg, the K2 = .8 (1) m = 0 .8 m

III. RESULTS

The results will be presented in photographs of site damage, in data tables, and in pressure-time records taken at various site locations and on the nonresponding model magazine.

A. Site Damage

Figures 8 - 10 illustrate the kind of damage that occurred to the responding model magazine. The donor magazine containing the 1 kg charge was destroyed completely. A crater was formed during each shot measuring 1.2 - 1.4 m across (measured to inside edge) and a depth of 0.26 to 0.28 m at the center. All craters were very similar from shot to shot.

The part of the barricade directly behind the donor charge model magazine was blown through on each shot. Both arms of the barricade on either side of the donor were crushed and moved away from the donor site (crater). The barricade behind and along the far side of the non-responding model was least disturbed of any part of the barricade. See Figures 9 and 10.

Figure 8-B illustrates the crushing and movement of the responding concrete model. Figure 8-C is a photograph of the reconstructed acceptor model showing the break-up of the various model components. The scored near side-wall did break as was anticipated, although the styrofoam witness plate (Figure 3-B) had almost no indentation from the movement of the wall segments. (The next series of tests planned will use velocity screens instead of the witness plate.)

B. Blast Loading on Acceptor Structure Near Side-Wall

Table 2 lists pertinent parameters at the three ground baffle stations. Station 19 is directly in front of the donor magazine. Station 20 is in front of the nonresponding acceptor model magazine, and Station 21 is on the other side of the barricade arm, past the nonresponding model. See Figures 4 - 6 above for the ground station locations for each of the three separation distances.

The peak pressures ranged from about 1500 kPa to 2300 kPa at Station 19 (where the distance remained the same) from 86 - 279 kPa at Station 20, and from 41 - 162 kPa at Station 21 over the three separation distances. For examples, see Figure 11.

Table 3 lists the parameters for the blast loading on the side-wall of the nonresponding model, nearest to the model donor magazine. Maximum values of reflected pressure peaks at Station 3 of about 900, 600, and 360 kPa were measured for separation distances of $0.8\ Q^{1/3}$ m, $1.6\ Q^{1/3}$ m, and $2.4\ Q^{1/3}$ m, respectively. Typical pressure-time waveforms are shown in Figures 12 and 13 for two representative stations, Stations 1 and 3. The

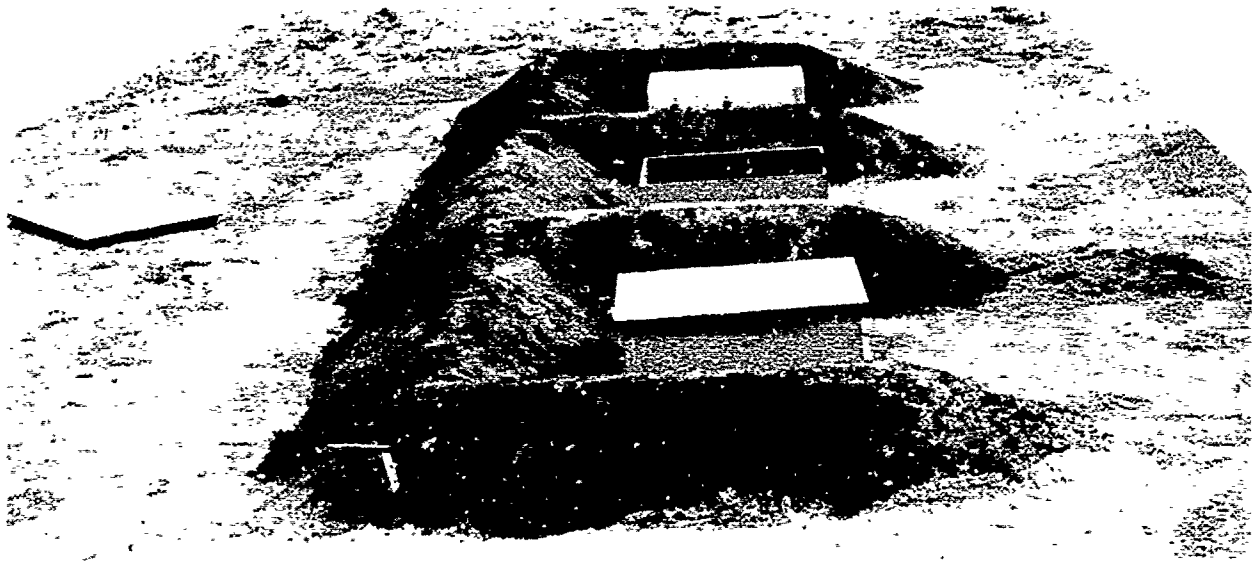

A. Preshot Site

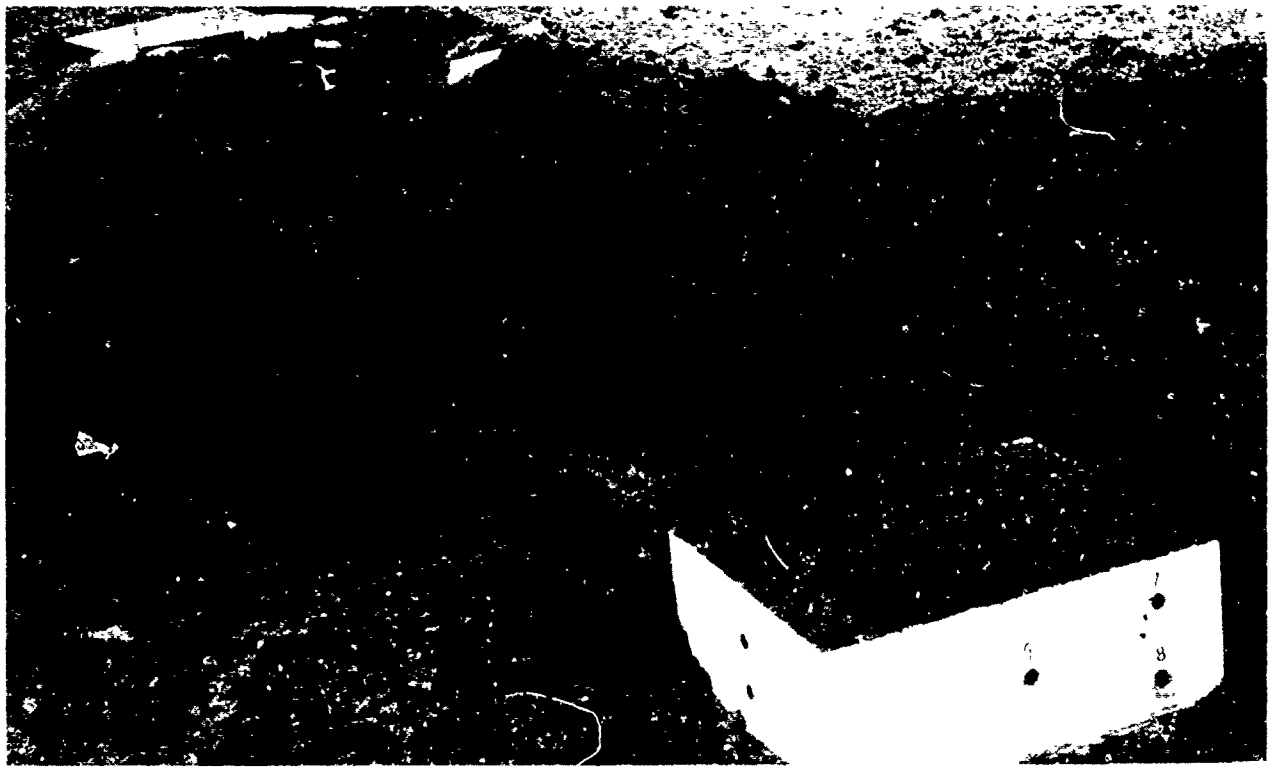

B. Postshot Site

Figure 8. Photographs for a Separation Distance of $0.8\ Q^{1/3}$ m (K2) 1695

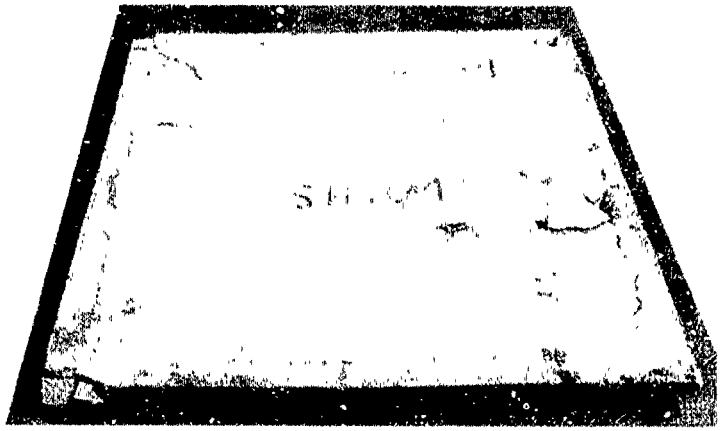

Roof

Back End Wall

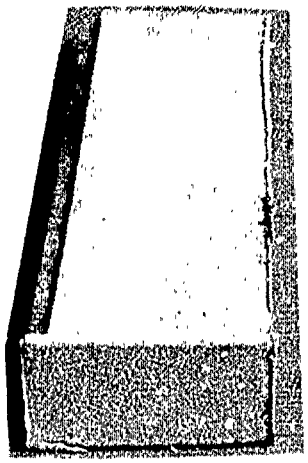

Far Wall

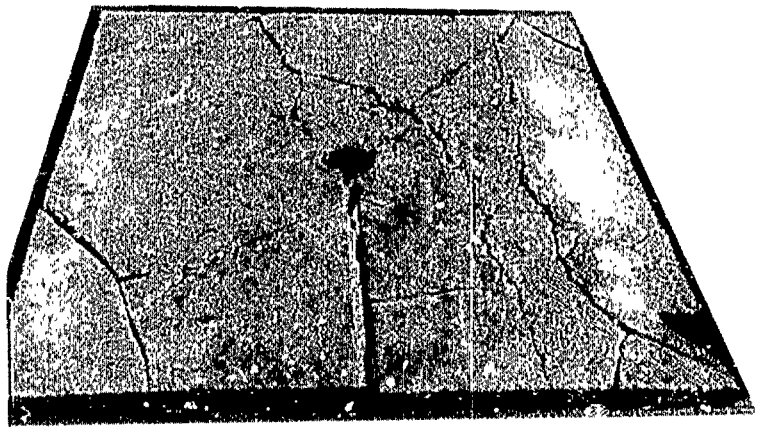

Floor

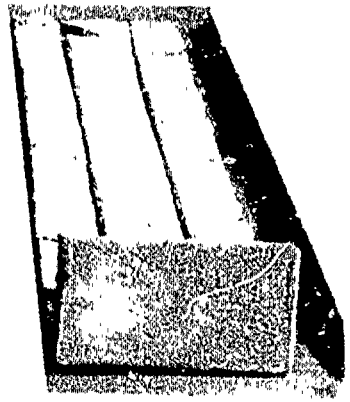

Near Wall

C. Postshot Acceptor Model Magazine

Figure 8. Photographs for a Separation Distance of $0.8\ Q^{1/3}$ m (K2) (Cont.)

A. Preshot Site

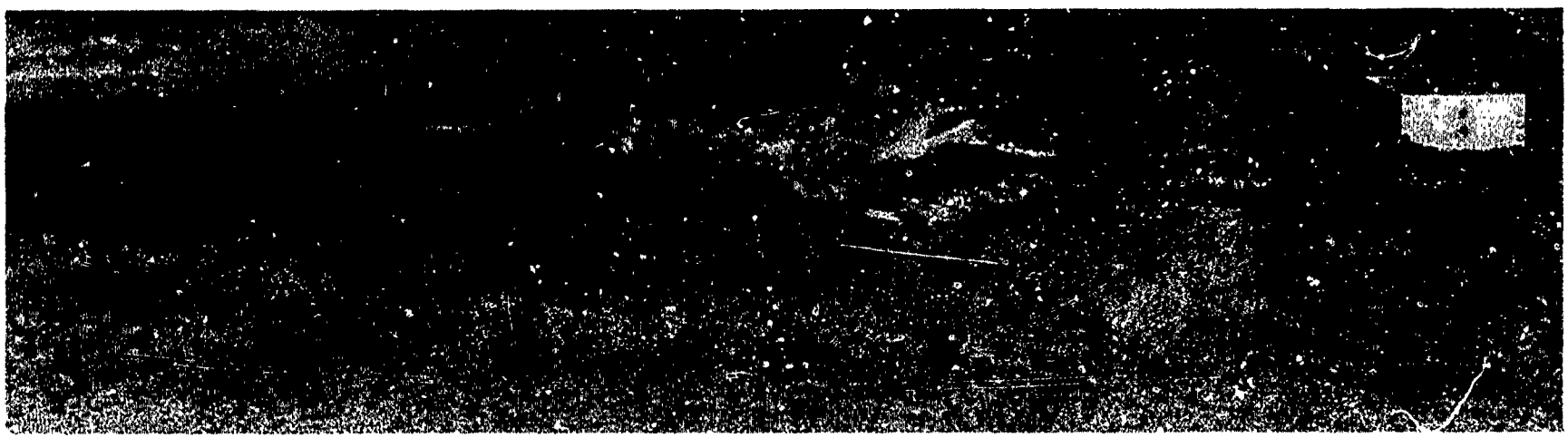

B. Postshot Site

Figure 9. Photographs for a Separation Distance of $1.6\ Q^{1/3}$ m (K4)

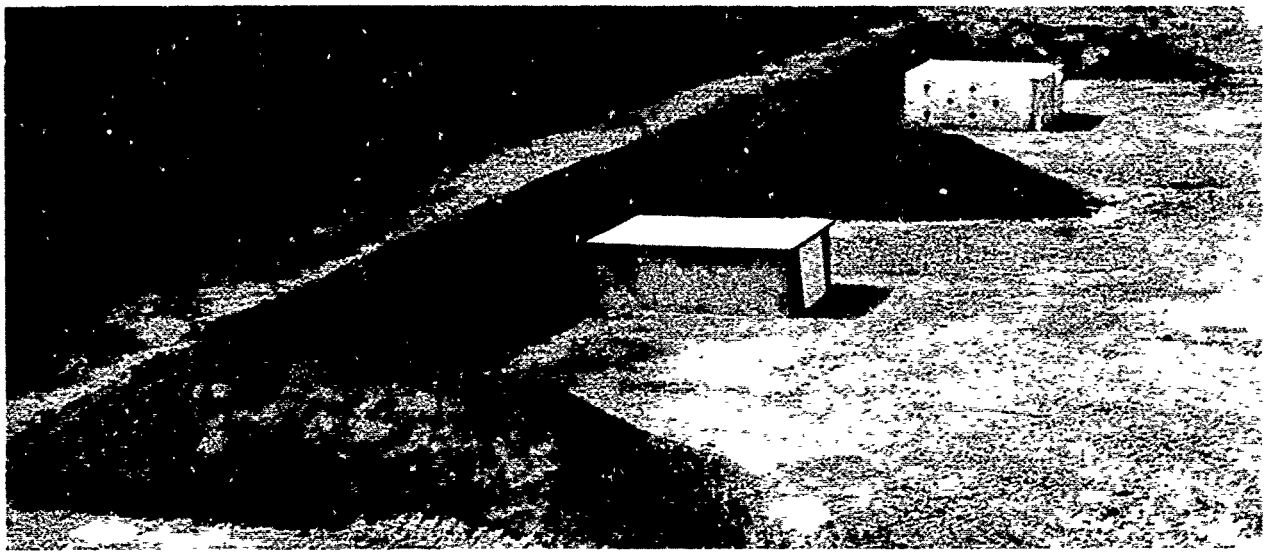

A. Preshot Site

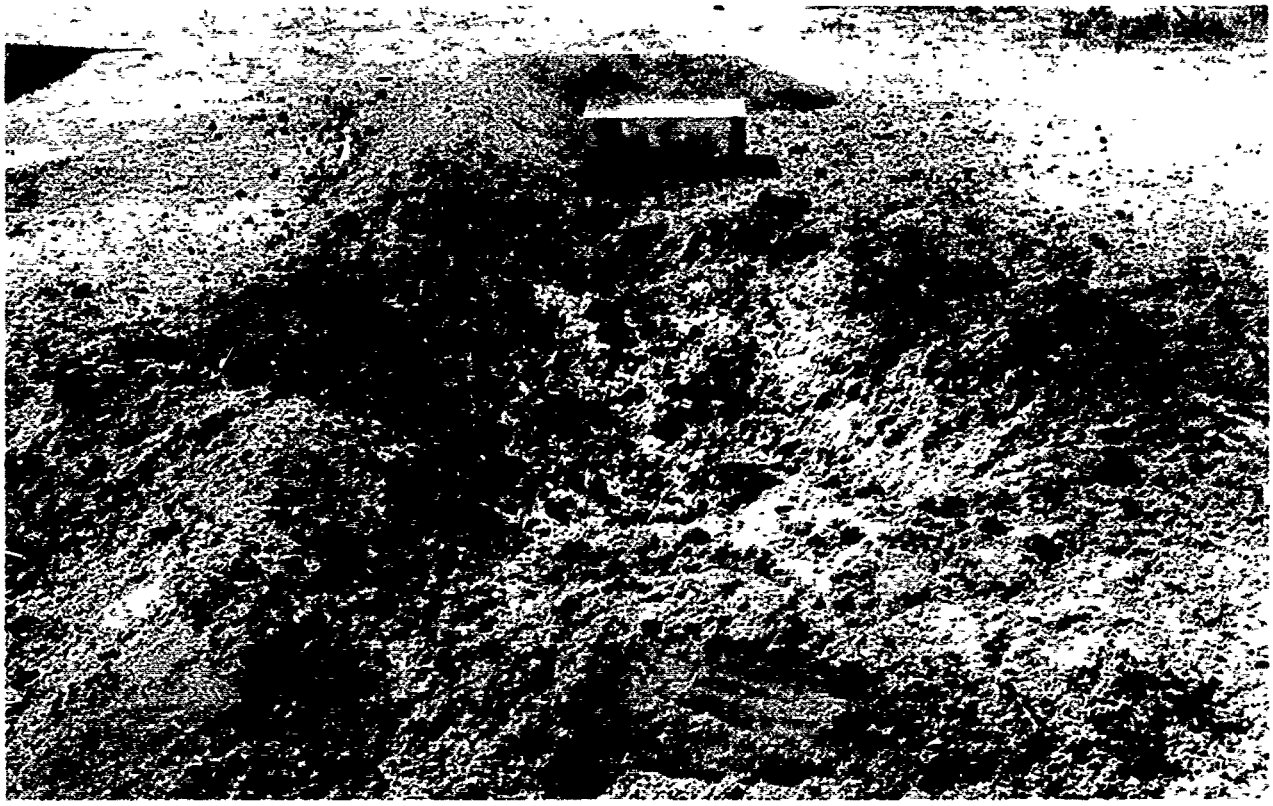

B. Postshot Site

Figure 10. Photographs for a Separation Distance of $2.4\ Q^{1/3}$ m (K6) 1698

TABLE 2. FREE-FIELD BLAST PARAMETERS-WITH BARRICADES

Shot	Station	Distance m	Peak Overpressure kPa	Impulse kPa-ms	Arrival Time ms	Duration ms	Remarks
1	19	1.006	1537	207	0.48	1.16	$0.8Q^{1/3}_m$
	20	1.523	279	97	1.34	1.41	
	21	2.286	162	88	3.24	1.66	
2	19	1.006	501/1575	238	0.46	1.04	$1.6Q^{1/3}$ m
	20	2.195	125	86	2.43	2.21	
	21	3.902	76	61	6.74	2.83	
3	19	1.006	2280	312	0.45	0.64	$1.6Q^{1/3}$ m
	20	2.195	143	89	2.43	2.00	
	21	3.902	67	60	6.77	2.82	
4	19	1.006	2147	229	0.45	0.50	$2.4Q^{1/3}$ m
	20	2.427	93	78	4.16	2.35	
	21	5.519	28.7	40	10.51	3.10	
5	19	1.006	667/1582	252	0.44	0.71	$2.4Q^{1/3}_m$
	20	2.427	95	81	4.15	2.43	
	21	5.519	43	48	10.49	3.56	
6	19	1.006	2032	226	0.44	0.67	$2.4Q^{1/3}$ m
	20	2.427	86	75	4.03	2.40	
	21	5.519	41	46	10.64	3.26	

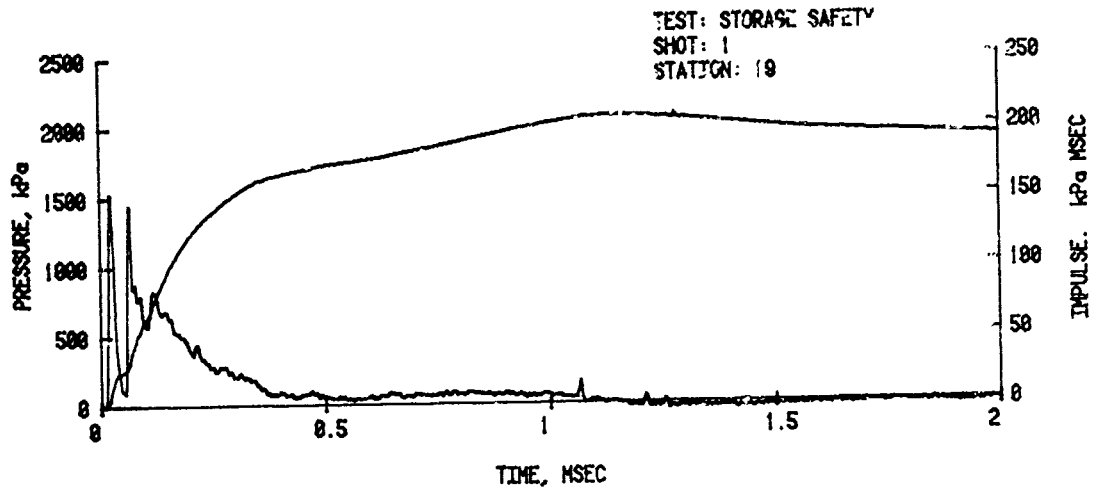

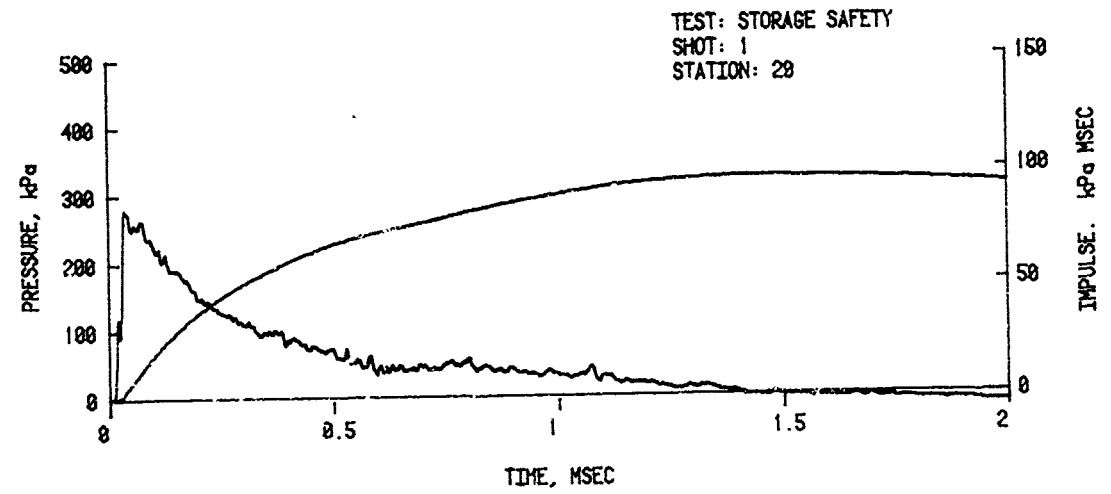

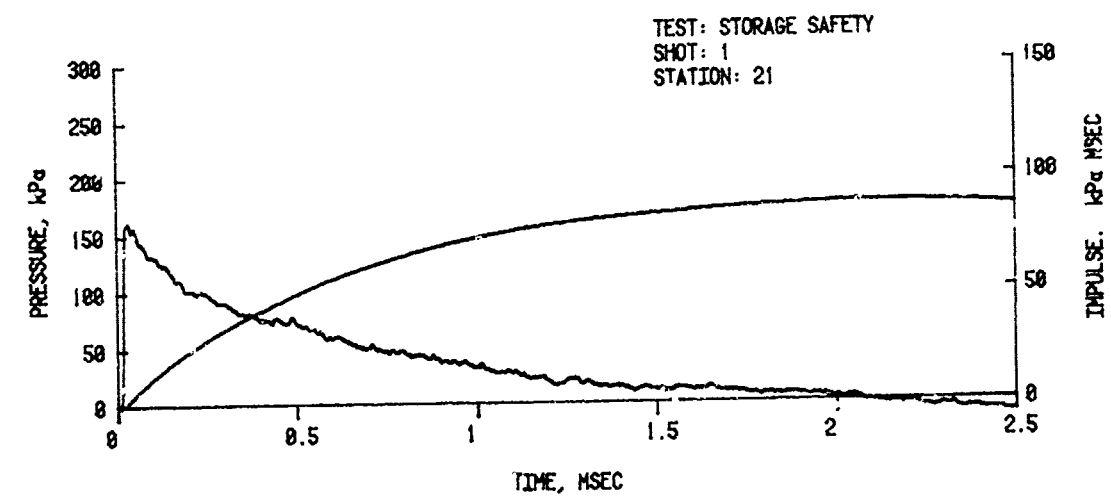

A. $0.8\ Q^{1/3}_m$

Figure 11. Pressure-Time Records, Free-Field with Barricades

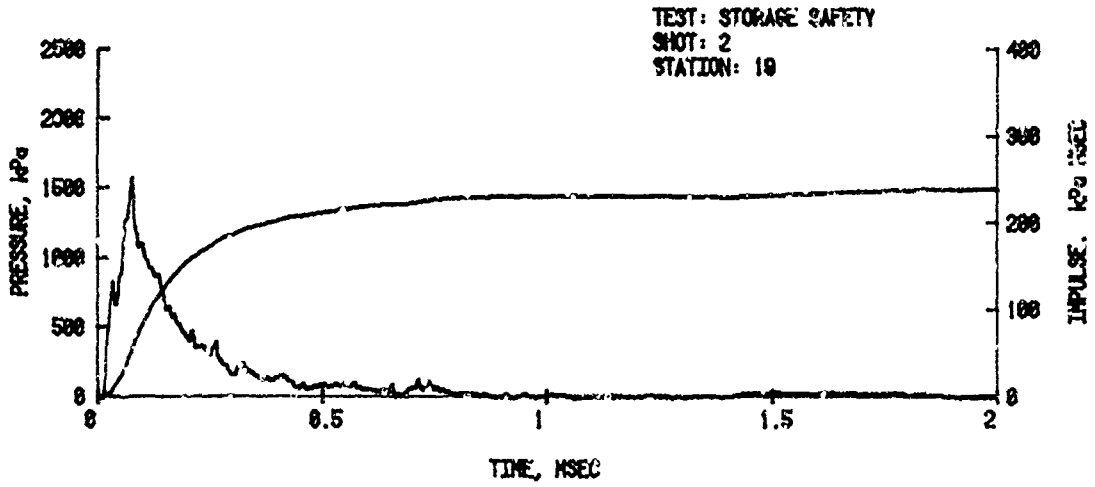

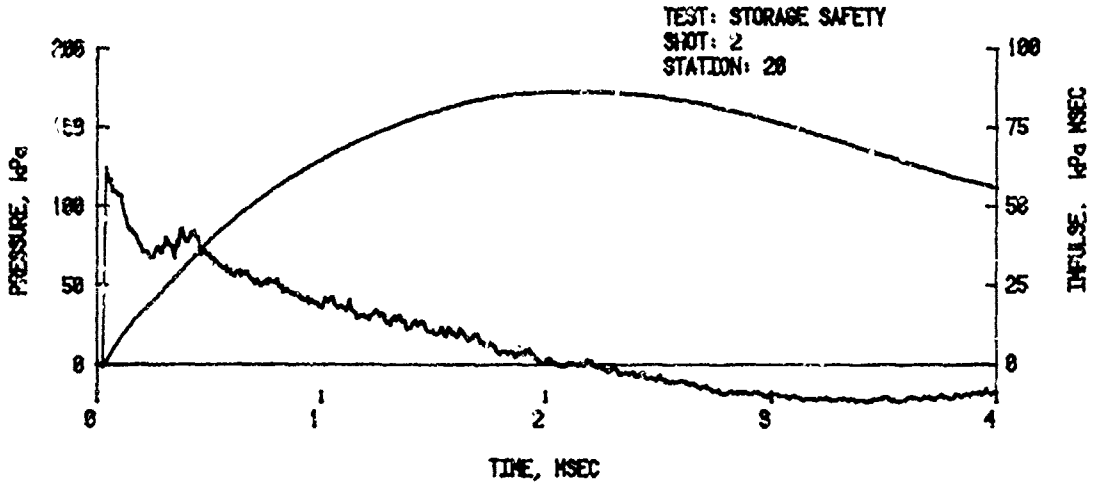

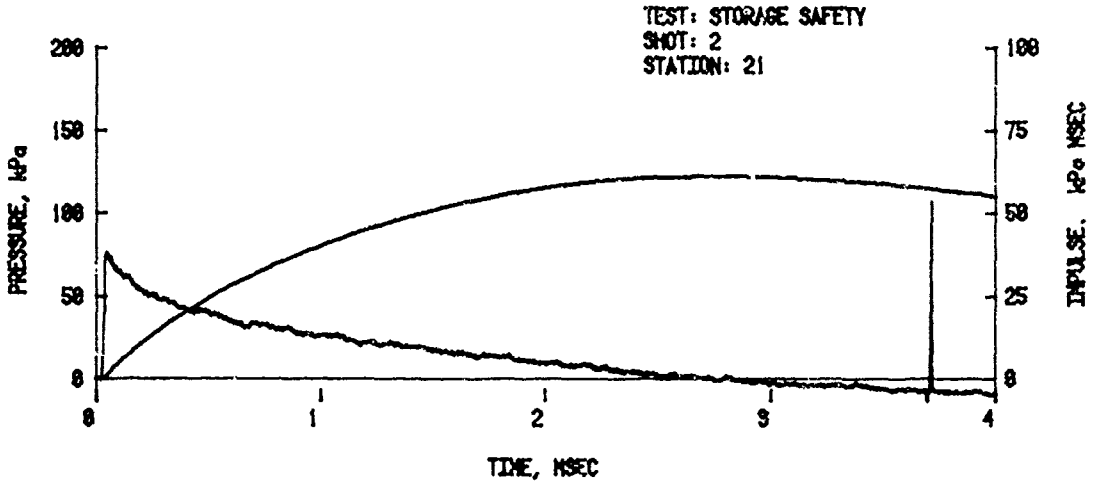

B. 1.6 $Q^{1/3}$ m

Figure 11. Pressure-Time Records, Free-Field with Barricades (Cont.)

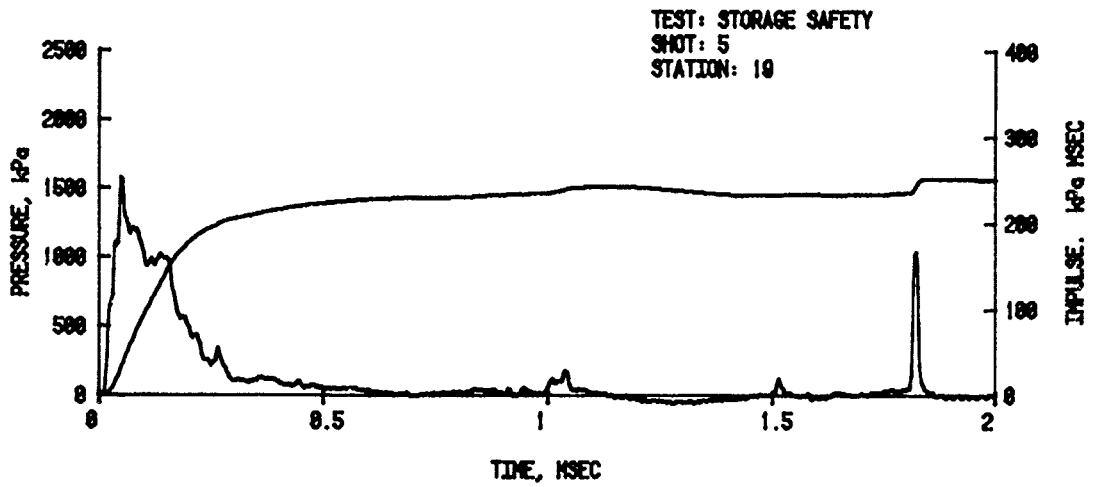

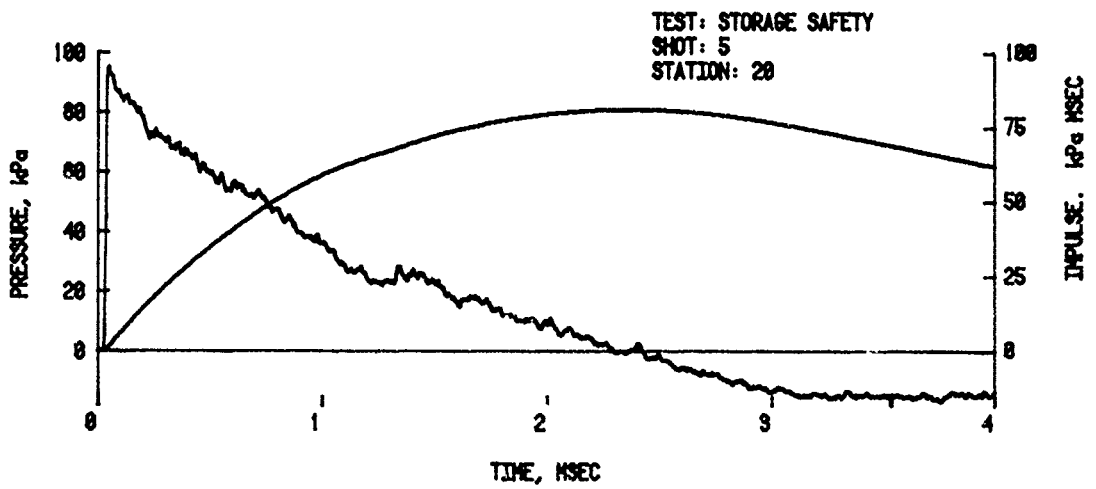

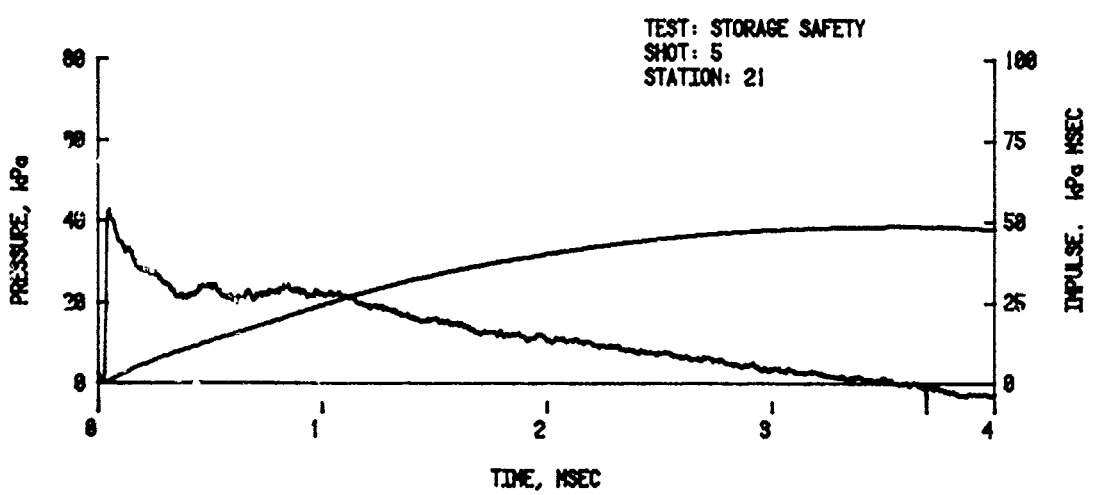

C. $2.4\ Q^{1/3}$ m

Figure 11. Pressure-Time Records, Free-Field with Barricades (Cont.)

TABLE 3. BLAST LOADING ON NEAR SIDE-WALL

Shot	Station	Peak Pressure kPa	Positive Impulse kPa-ms	Arrival Time ms	Positive Duration ms	Remarks
1	1	1128	182	0.80	0.56	$0.8Q^{1/3}$ m
	2	814/1707*	253	0.85	0.56	
	3	890	205	0.82	0.61	
	4	894	187	0.83	0.69	
	5	815	239	0.84	0.59	
	6	-	-	-	-	
2	1	300/565	165	1.96	1.13	$1.6Q^{1/3}$ m
	2	797/812	209	2.00	0.97	
	3	284/578	197	1.98	0.92	
	4	354/459	195	1.95	0.94	
	5	658	206	1.99	0.81	
	6	339/580	213	1.97	1.02	
3	1	339/513	156	1.88	1.17	$1.6Q^{1/3}$ m
	2	726	194	1.93	1.04	
	3	-	-	-	-	
	4	357/373	180	1.87	1.00	
	5	321/578	210	1.93	0.88	
	6	358/554	198	1.91	1.01	
4	1	488	125	3.40	1.89	$2.4Q^{1/3}$ m
	2	399/420	142	3.41	1.86	
	3	343/349	137	3.40	1.97	
	4	366	138	3.38	2.00	
	5	414/428	164	3.41	1.79	
	6	440	144	3.39	2.00	
5	1	319/416	119	3.49	1.58	$2.4Q^{1/3}$ m
	2	299/356	133	3.49	1.11	
	3	304/369	133	3.49	1.26	
	4	472	142	3.48	2.00	
	5	288/391	144	3.49	0.98	
	6	306/420	145	3.49	2.00	
6	1	243	106	3.40	1.96	$2.4Q^{1/3}$ m
	2	246	116	3.40	1.78	
	3	240	112	3.40	1.72	
	4	264	119	3.40	1.82	
	5	256/263	124	3.41	1.66	
	6	270	123	3.41	1.64	

*Second value refers to maximum reflected pressure peak if the initial peak is not the maximum.

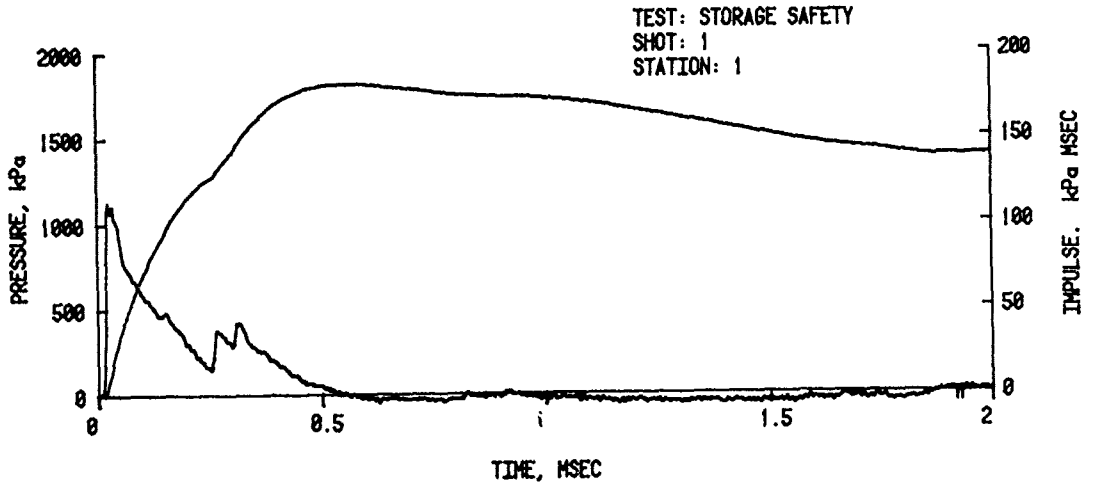

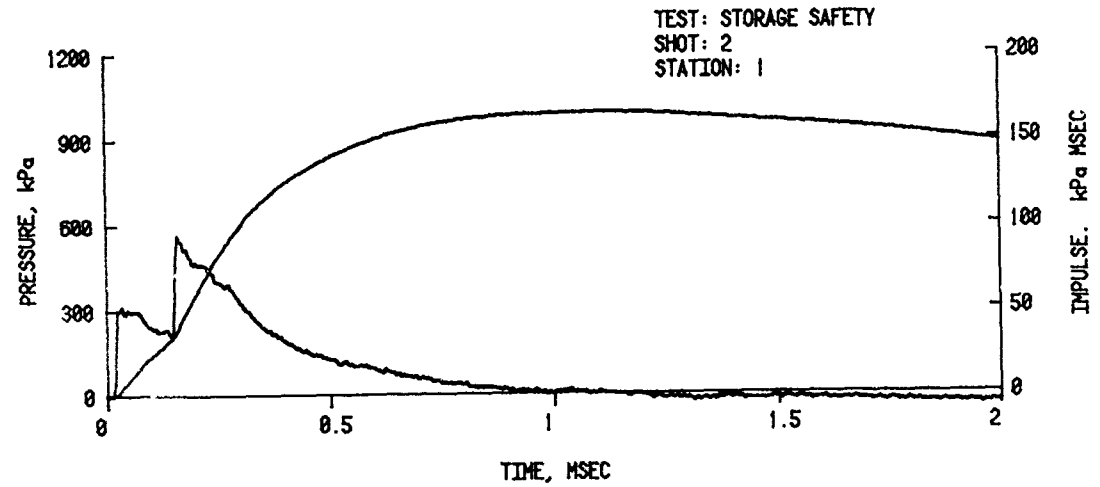

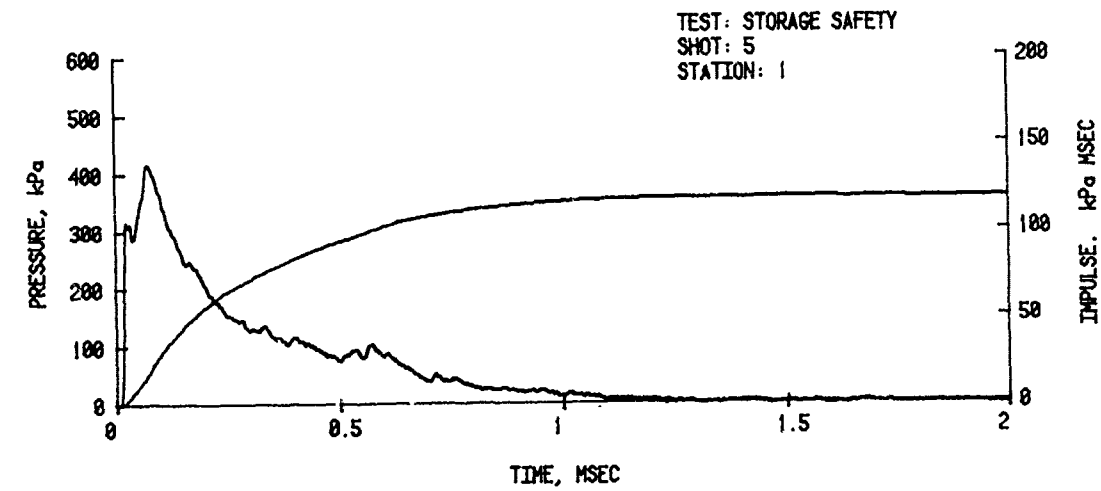

Figure 12. Pressure-Time Records from Near Side-Wall, Station 1

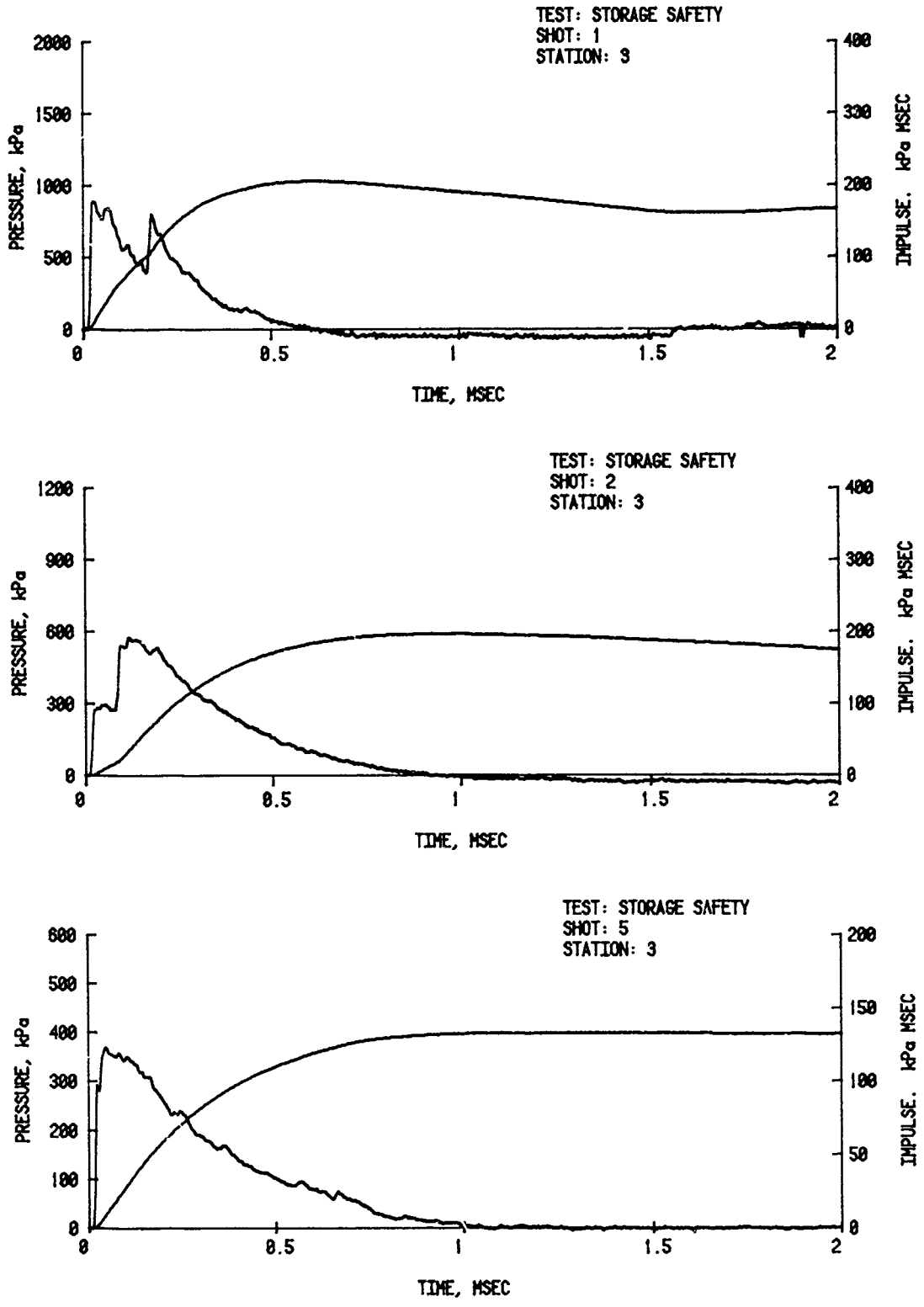

Figure 13. Pressure-Time Records from Near Side-Wall, Station 3

waveform change as a function of separation distance is shown by the variation in peak formation: a large initial peak, a small initial peak and finally almost a single peak again. It should be pointed out that the difference in wave shapes at Stations 1 and 3 as shown in Figures 12 and 13 is because of the Mach reflection process where the reflection wave is catching up to the incidence shock as the distance from ground zero increases.

C. Blast Loading on Acceptor Structure - Roof

Table 4 lists the blast loading parameters for the roof of the acceptor model. Maximum values of about 480, 170, and 180 kPa were recorded at Station 13 for the three separation distances. Figures 14 - 16 are examples of the pressure-time curves recorded from Stations 13, 14, and 16. The waveforms are quite similar (for a specific shot) with some decay of peak pressure during the crossing of the roof.

D. Blast Loading on Acceptor Structure - Ends

Maximum peak pressure is seen to occur (Table 5) at Station 11 with a variation of about 500, 195, and 120 kPa corresponding to the three separation distances. The waveforms are shown in Figures 17 and 18. The general shape of the records from both ends of the acceptor magazine are quite similar, as were those on the roof.

E. Blast Loading on Acceptor Structure - Far Side-Wall

Table 6 lists the maximum peak pressure as measured on the far side-wall of the acceptor magazine. The values ranged from about 200 kPa for Station 9 at a distance of $0.8\ Q^{1/3}$ m to a low of about 62 kPa at a distance of $2.4\ Q^{1/3}$ m.

Figures 19 and 20 illustrate the variety of waveforms to be found on the far side-wall. A great many small reflections were recorded at the outer edge at Station 8 during Shot 1. At Station 9, near the center of the wall, large distinct reflections from the ground surface and the barricade were recorded for all three separation distances. No record approached the maximum pressure level measured on the near side-wall, however.

TABLE 4. BLAST LOADING ON ROOF

Shot	Station	Peak Pressure kPa	Positive Impulse kPa-ms	Arrival Time ms	Positive Duration ms	Remarks
1	12	418	99	0.84	0.86	$0.8Q^{1/3}$ m
	13	481	120	0.84	0.92	
	14	397	108	0.99	1.07	
	15	273	91	1.18	1.55	
	16	350	105	1.16	1.32	
2	12	143/147	62	2.03	0.70	$1.Q^{1/3}$ m
	13	146/149	63	2.03	0.70	
	14	152	91	2.25	1.32	
	15	125/141	78	2.51	1.86	
	16	140	80	2.49	1.92	
3	12	158	70	1.95	1.63	$1.6Q^{1/3}$ m
	13	169	74	1.97	0.80	
	14	148/160	84	2.18	1.41	
	15	125	75	2.43	2.00	
	16	128	72	2.41	1.96	
4	12	161	52	3.51	1.60	$2.4Q^{1/3}$ m
	13	39/156	50	3.45	0.90	
	14	35/146	71	3.64	2.52	
	15	126	70	3.94	2.76	
	16	135	73	3.84		
5	12	162	56	3.59	1.98	$2.4Q^{1/3}$ m
	13	179	58	3.58	0.91	
	14	149	73	3.79	2.59	
	15	136	66	4.04	2.59	
	16	166	68	4.02	2.61	
6	12	92/101	65	3.51	1.91	$2.4Q^{1/3}$ m
	13	103	54	3.52	1.24	
	14	93	71	3.76	2.51	
	15	77	64	4.04	2.58	
	16	88	67	4.02	2.51	

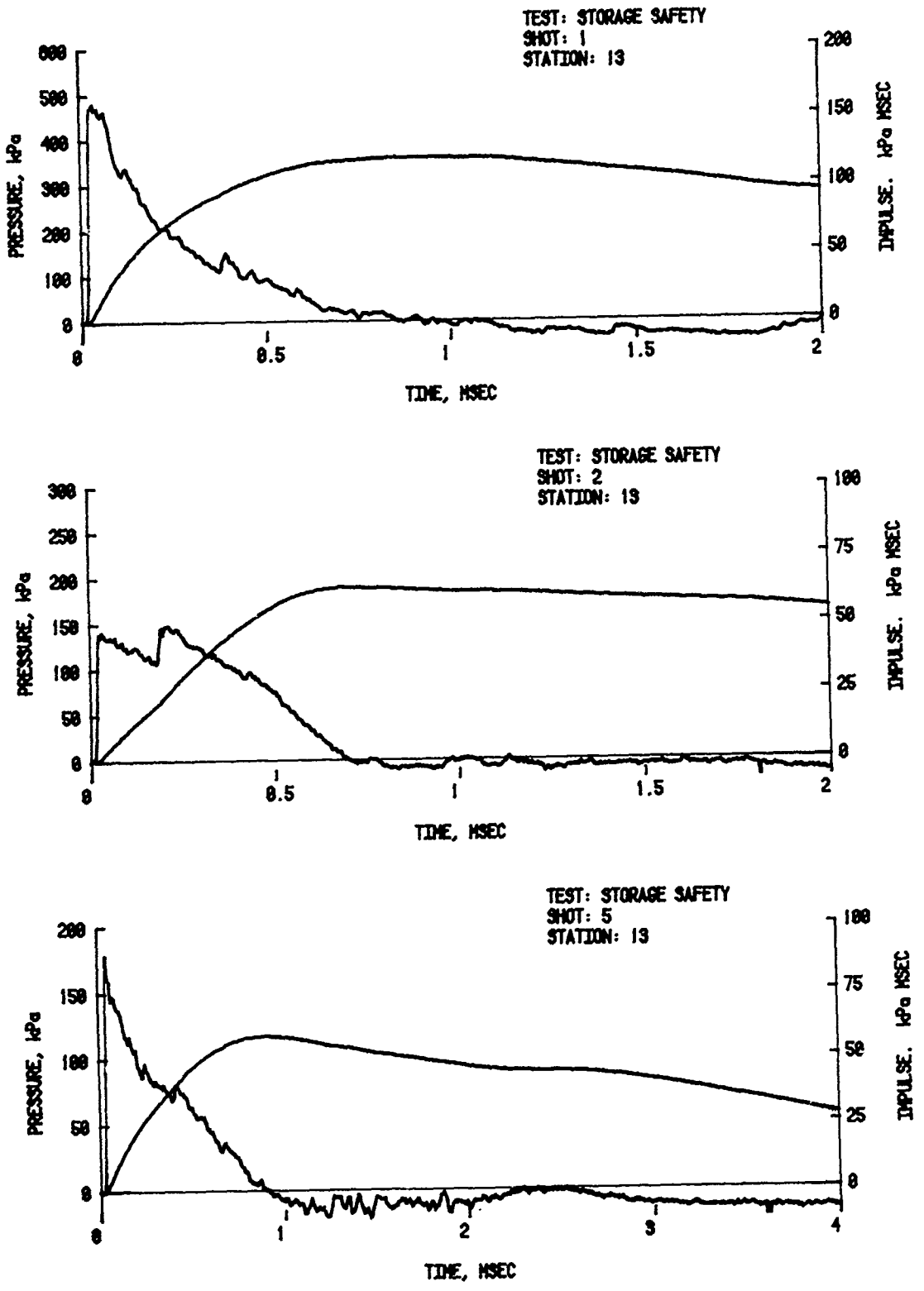

Figure 14. Pressure-Time Records from the Roof, Station 13

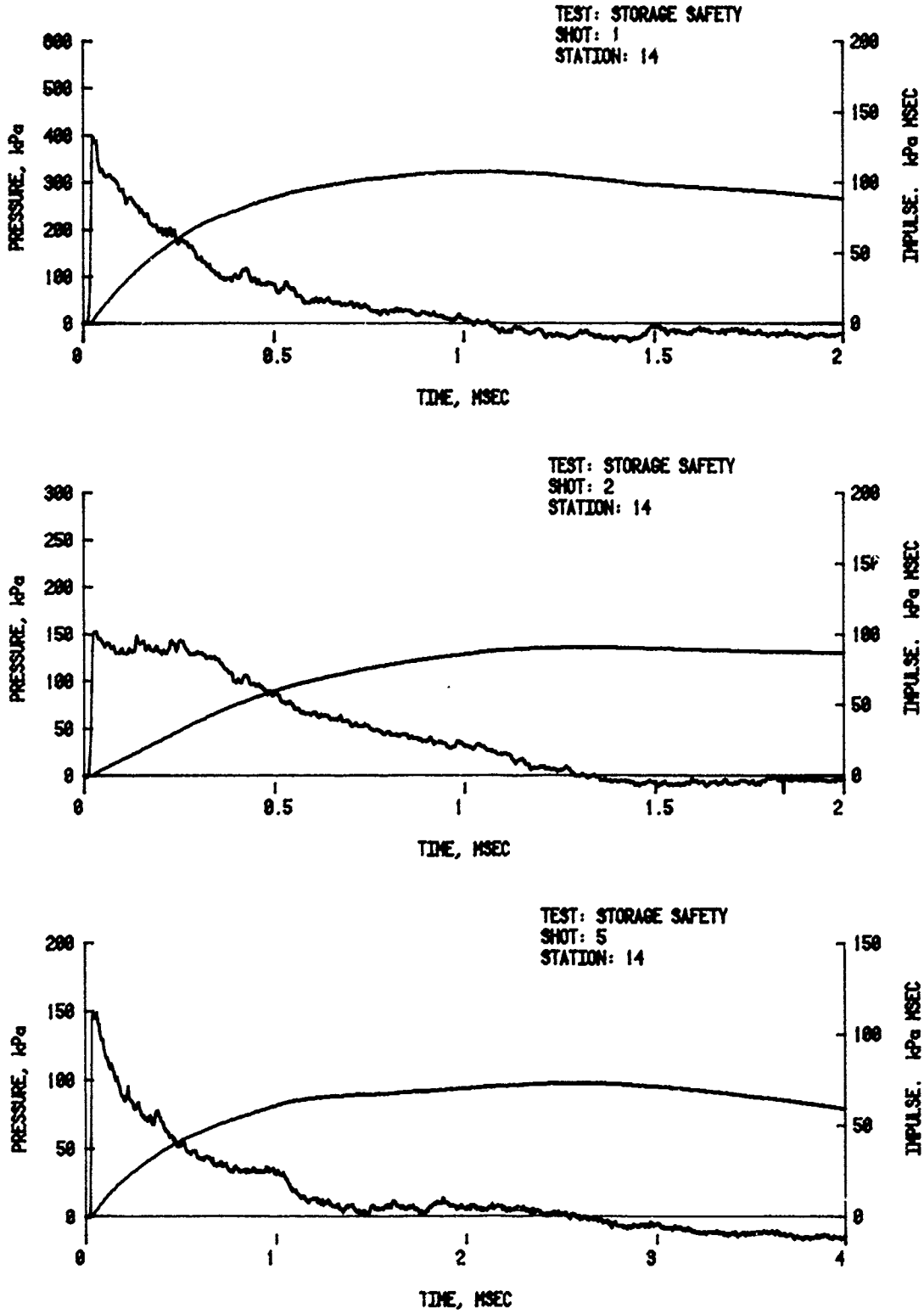

Figure 15. Pressure-Time Records from the Roof, Station 14

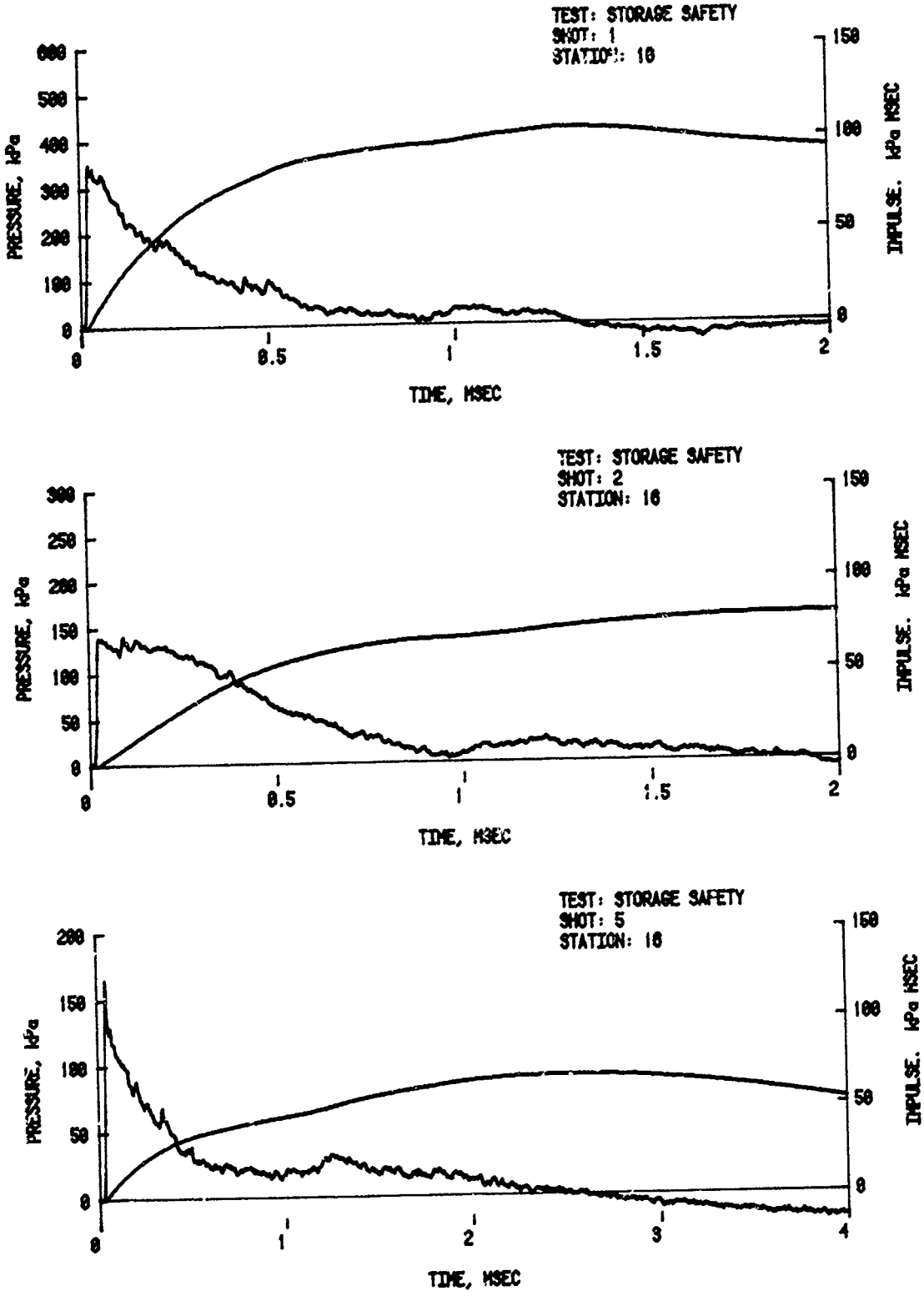

Figure 16. Pressure-Time Records from the Roof, Station 16

Table 5. BLAST LOADING ON END WALLS

Shot	Station	Peak Pressure kPa	Positive Impulse kPa-ms	Arrival Time ms	Positive Duration ms	Remarks
1	10	240/478	104	1.06	0.99	$0.8Q^{1/3}$ m
	11	518	114	1.10	0.83	
	17	242/297	105	1.08	1.27	
	18	332	108	1.10	1.22	
2	10	189	88	2.29	1.37	$1.6Q^{1/3}$ m
	11	172/184	94	2.32	1.41	
	17	170	96	2.30	1.48	
	18	145/167	91	2.29	1.44	
3	10	188	81	2.22	1.33	$1.6Q^{1/3}$ m
	11	195	83	2.24	1.26	
	17	186	94	2.26	1.47	
	18	167	91	2.25	1.41	
4	10	117	70	3.76	2.36	$2.4Q^{1/3}$ m
	11	129	94	3.82	4.00	
	17	116	74	3.81	2.46	
	18	117	81	3.82	2.61	
5	10	127	72	3.85	2.85	$2.4Q^{1/3}$ m
	11	96/120	67	3.88	1.83	
	17	133	78	3.87	2.27	
	18	95/115	81	3.86	2.42	
6	10	84	64	3.77	2.48	$2.4Q^{1/3}$ m
	11	81	75	3.79	2.72	
	17	93	71	3.80	2.02	
	18	90	71	3.79	2.42	

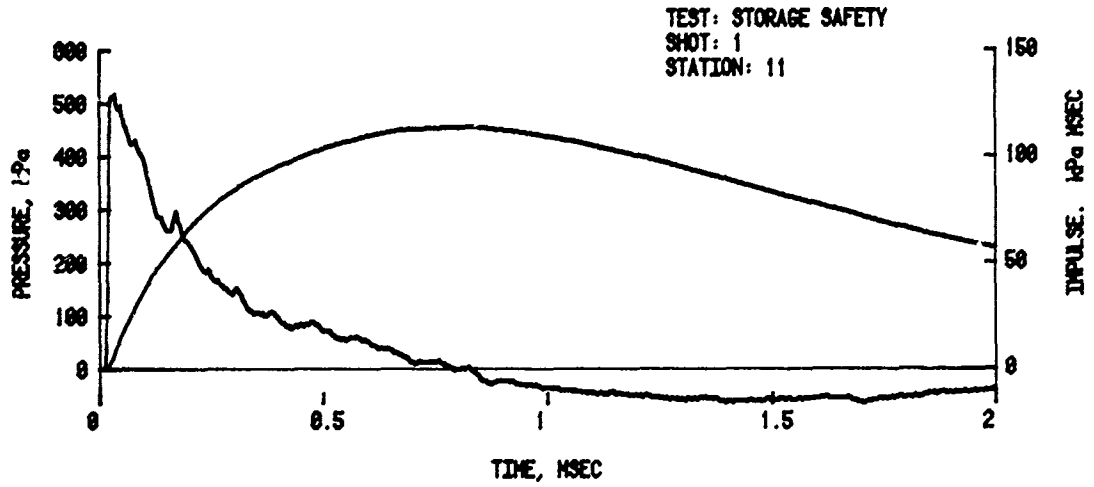

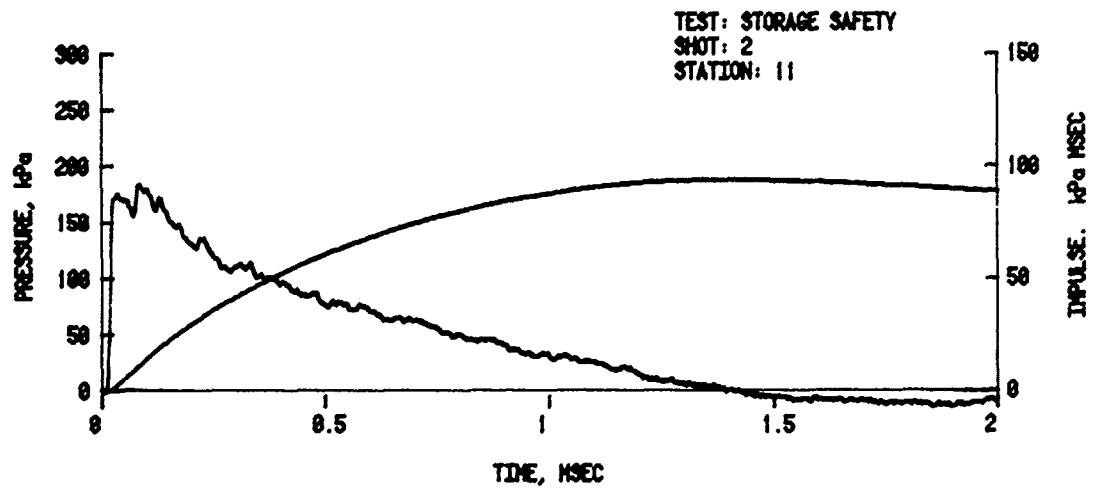

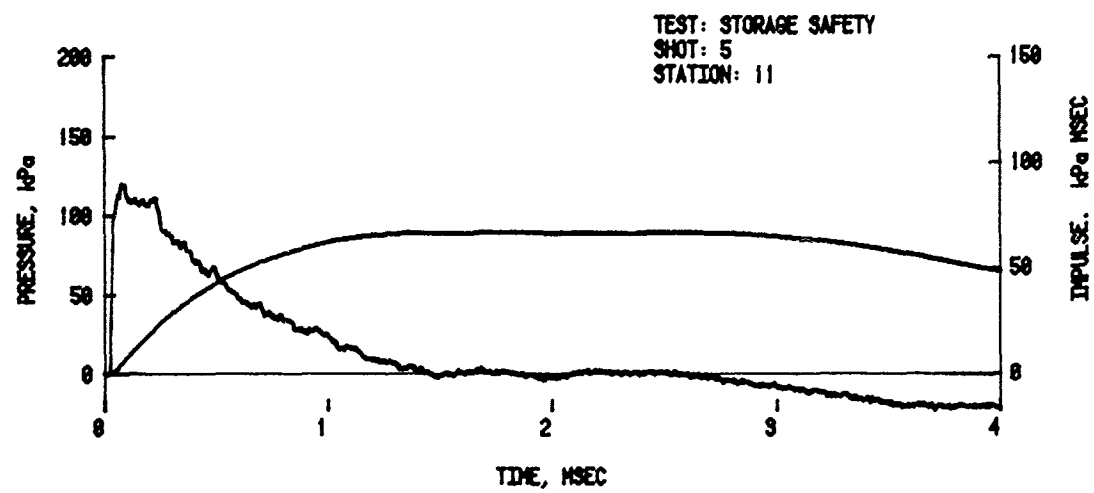

Figure 17. Pressure-Time Records from Back End-Wall, Station 11

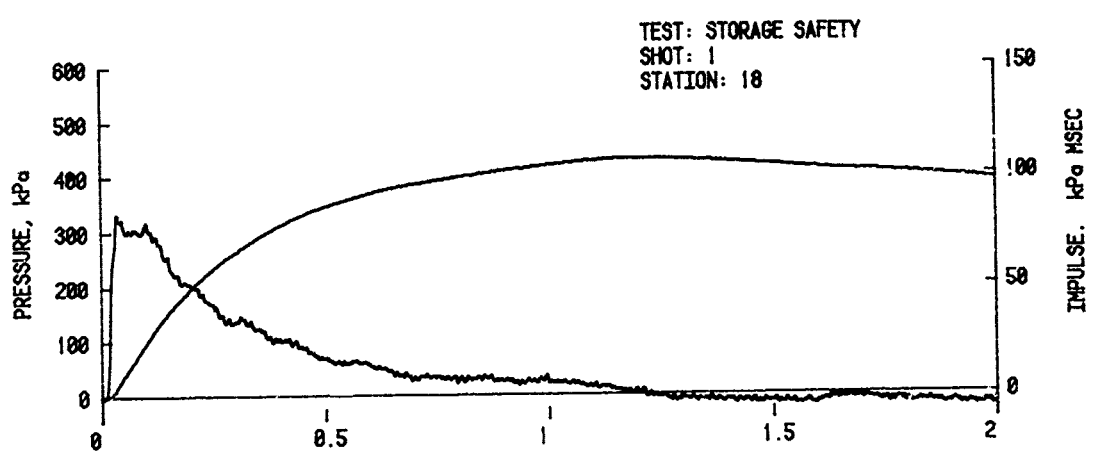

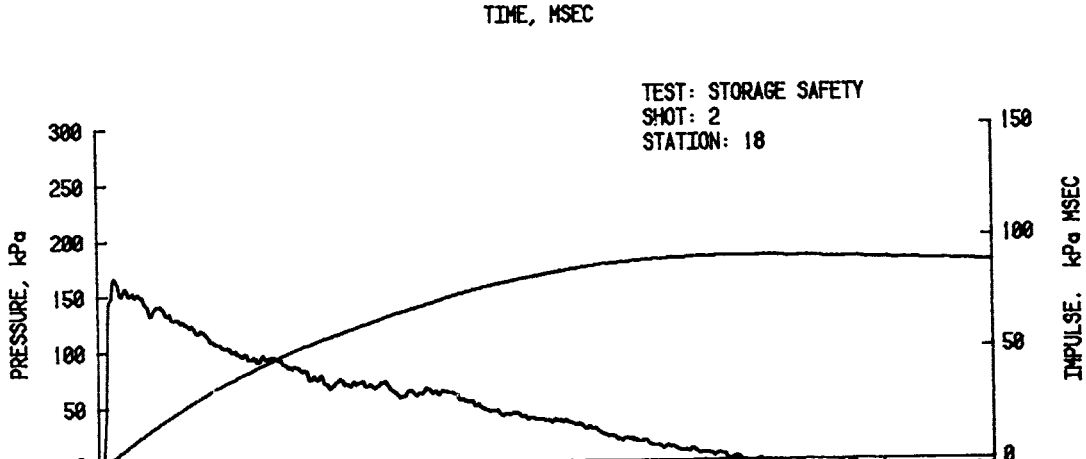

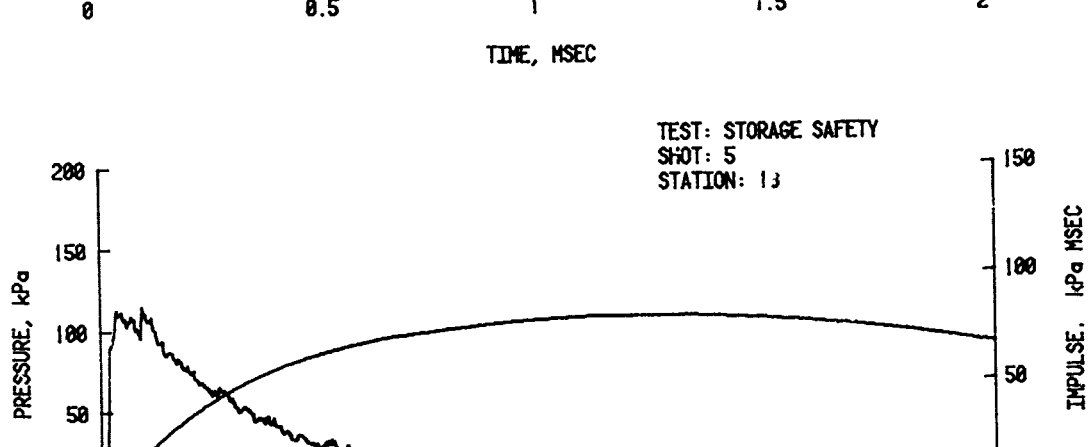

Figure 18. Pressure-Time Records from Front End Wall, Station 18

Table 6. BLAST LOADING ON FAR SIDE-WALL

Shot	Station	Peak Pressure kPa	Positive Impulse kPa-ms	Arrival Time ms	Positive Duration ms	Remarks
1	7	63/81	70	1.33	1.85	$0.8Q^{1/3}$ m
	8	83/141	117	1.47	1.75	
	9	65/198	114	1.42	1.70	
2	7	27/64	30	2.70	1.68	$1.6Q^{1/3}$ m
	8	34/73	67	2.79	3.16	
	9	44/80	80	2.79	3.07	
3	7	34/61	32	2.62	1.71	$1.6Q^{1/3}$ m
	8	34/64	78	2.72	3.18	
	9	39/87	82	2.72	3.18	
4	7	28/42	59	4.09	2.49	$2.4Q^{1/3}$ m
	8	61	62	4.29	2.58	
	9	28/62	60	4.12	2.65	
5	7	31/43	56	4.23	2.85	$2.4Q^{1/3}$ m
	8	27/63	66	4.39	2.82	
	9	36/83	68	4.32	2.80	
6	7	18/42	61	4.24	2.89	$2.4Q^{1/3}$ m
	8	14/46	61	4.34	2.60	
	9	8.6/62	57	4.34	2.47	

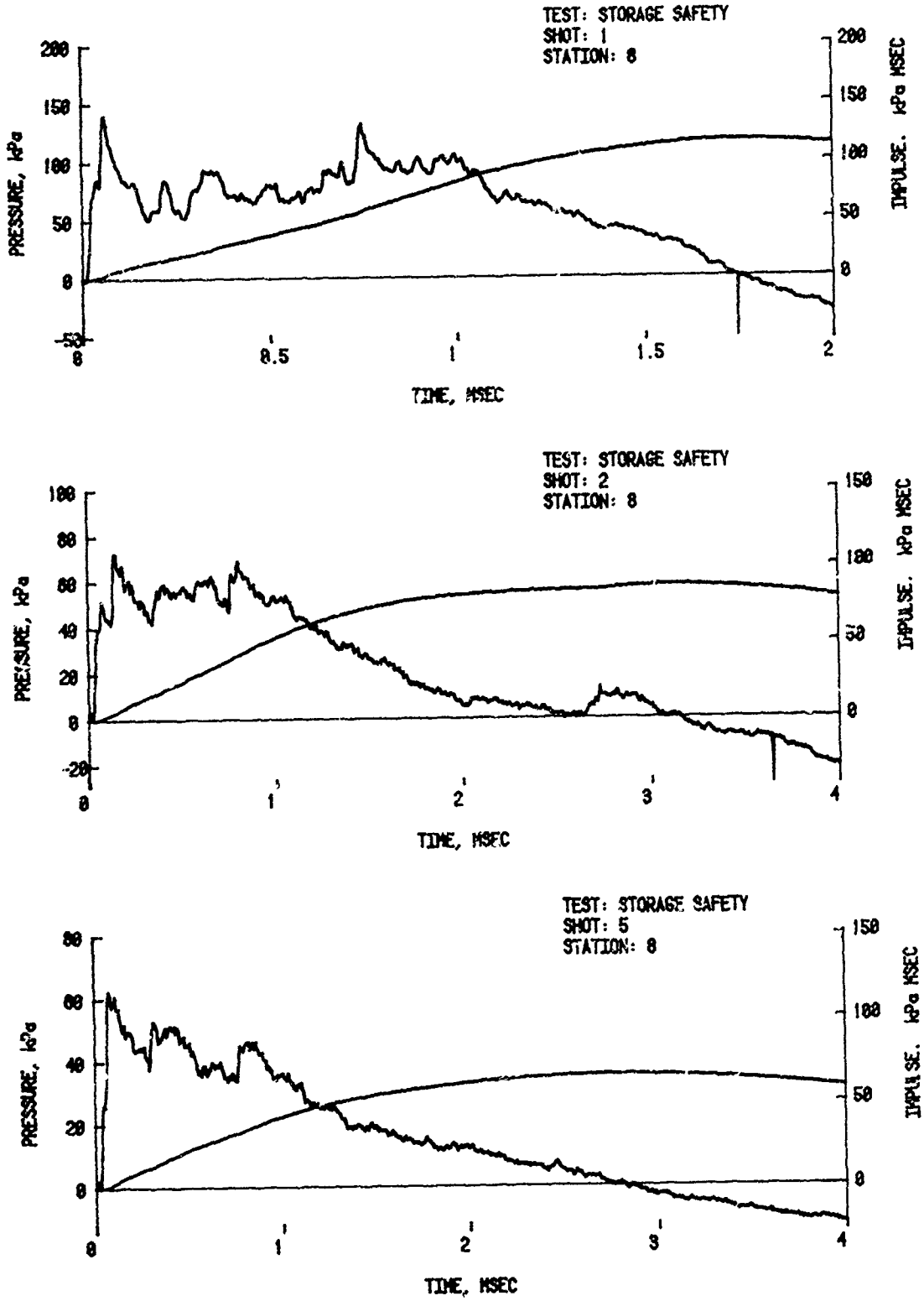

Figure 19. Pressure-Time Records from Far Side-Wall, Station 8

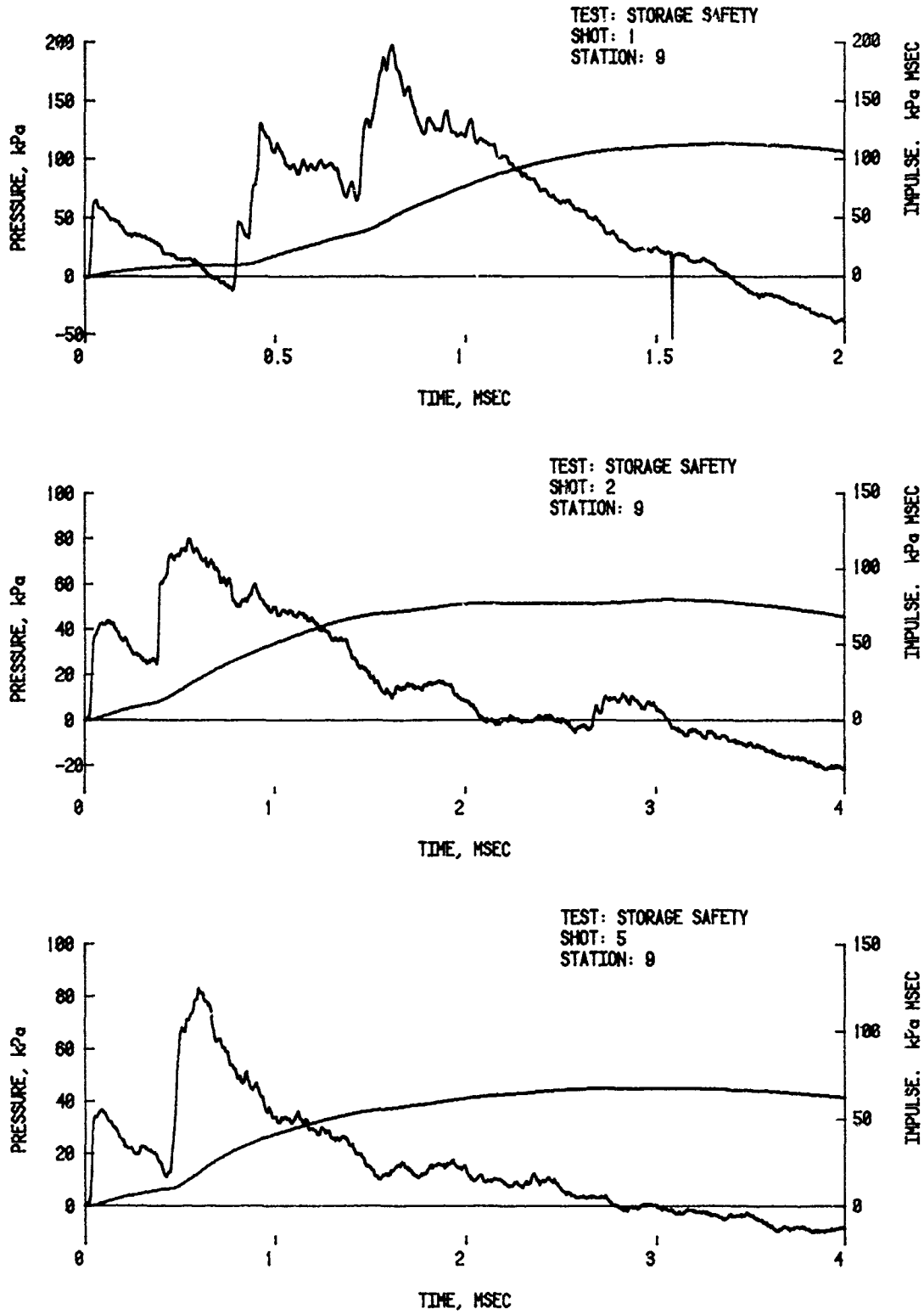

Figure 20. Pressure-Time Records from Far Side-Wall, Station 9

IV. ANALYSIS

A. Blast Suppression Factors

The blast wave from the charge inside the donor magazine is suppressed to the sides and to the rear by both the presence of the cover and also the barricades. The cover effect is similar to that for a cased charge. Reference 1 gives an expression for a case correction factor, fc, which will be used for the cover effect of the donor structure.

$$fc = 0.02 + \frac{0.80}{1 + (W_{CT}/W_{NEW})}, \tag{1}$$

where W_{CT} is the total case weight (donor structure cover) and W_{NEW} is the net explosive weight. For an average value of 5.566 kg for W_{CT} and 1 kg for W_{NEW}, fc is found from Equation 1 to be 0.321 kg.

The equivalent TNT weight, W_{TNT}, for a Pentolite charge and the donor structure is found from Equation 2.

$$W_{TNT} = fc \times fe \times W_{NEW}, \tag{2}$$

where the case factor, fc, is taken as 0.321 and the pressure equivalent explosive weight factor, fe, for Pentolite is 1.17 from Reference 3. The equivalent base TNT weight, W_{TNT}, is 0.375 kg of TNT, from Equation 2.

Alternate comparisons of the suppressive effects may be made by comparing the measured parameters at Station 20 (in front of the acceptor magazine model) with the free-field values from the stardard curves for hemispherical TNT detonated on a hard surface. See References 4 and 5 for the scaling rules. The scaling rule used is given in Equation 3 for the charge mass-distance relationship. At a given peak overpressure

$$Q_2 = Q_1 \left(\frac{R_2}{R_1}\right)^3, \tag{3}$$

where R_1 is the distance from Q_1 (1 kilogram of explosive)

and R_2 is the distance from Q_2 (the equivalent mass of bare TNT needed to give the experimentally suppressed values for a 1 kilogram charge inside the donor magazine model).

The values of R_1 and R_2 are read from Figure 21A for Station 20 and 21B for Station 21. These are listed in Table 7 with the equivalent bare charge mass Q_2 . The average value for Q_2 of 0.43 at Station 20 compares quite well with the value of 0.38 calculated from Equation 2. It can be seen in Figure 21B that the suppressive effect is not evident at Station 21. The average value of Q_2 at Station 21 is 1.02 which implies no suppression of peak overpressure.

As noted in Reference 2 the impulse in the blast wave from the covered donor does not produce the same Q_2 values when standard scaling procedures are used. To determine the Q_2 based on impulse the following procedure was used.

A ratio of experimental values I_2/R_2 from Table 2 are determined for each shot. These are plotted along with the standard impulse/distance (I_1/R_1) versus distance curve in Figure 22. For a ratio of I_1/R_1 equal to I_2/R_2, an R_1 is found. The values of R_2 and R_1 found in this way may now be put into Equation 3 to calculate Q_2. These ratios of impulse and distance, and Q_2 values for Stations 20 and 21 are listed in Table 8. It can be seen that the Q_2 values for impulse are quite different from the Q_2 values calculated from the suppression of peak overpressure. The Q_2 values are also different for the two station locations. Table 8 can be summarized by stating that the impulse at Station 20 from a 1 kg covered donor can be matched with a 0.56 bare charge, and at Station 21 would require a 0.72 kg charge.

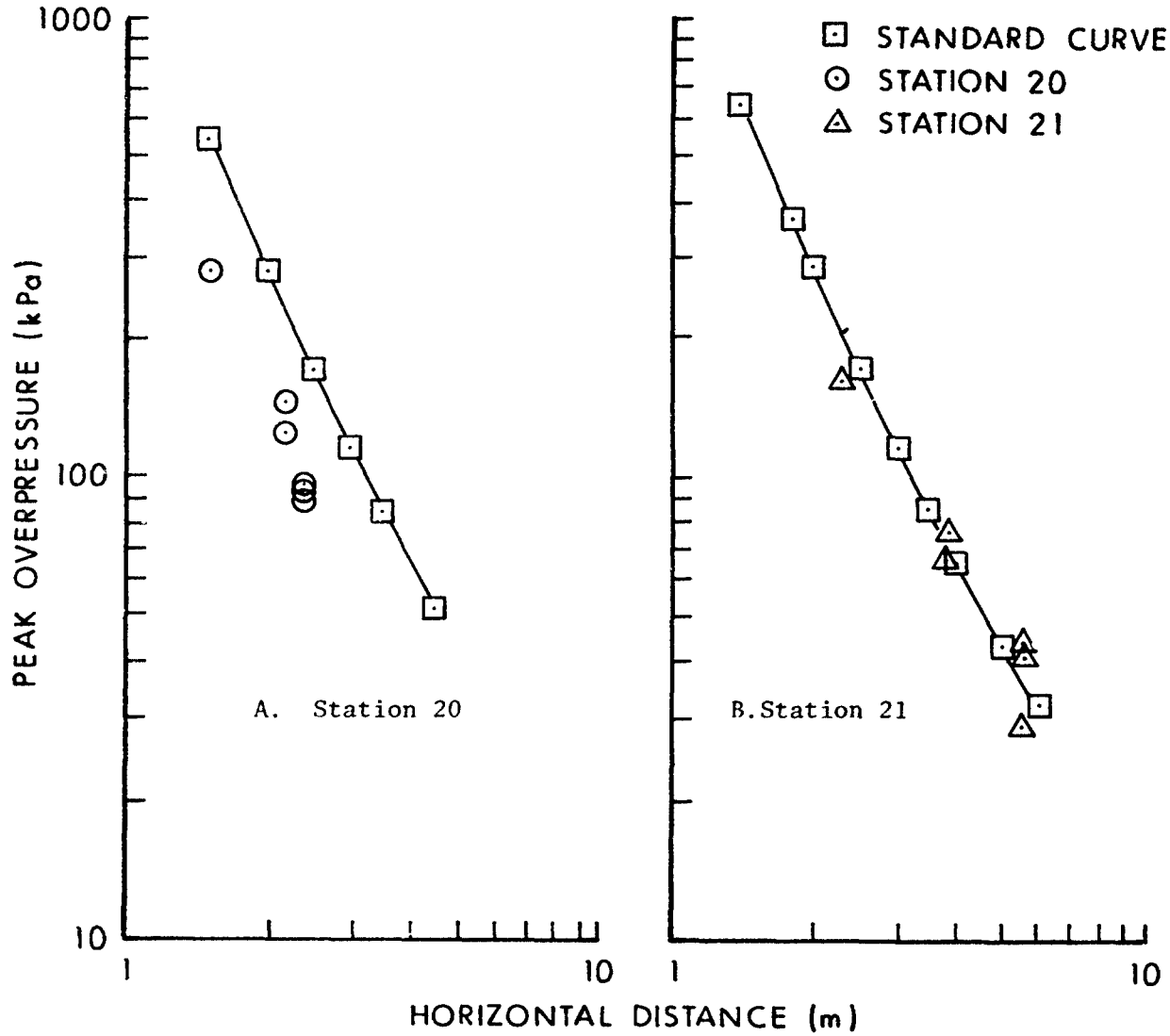

Figure 21. Comparison of Standard Free-Field Pressures to Data from Stations 20 and 21.

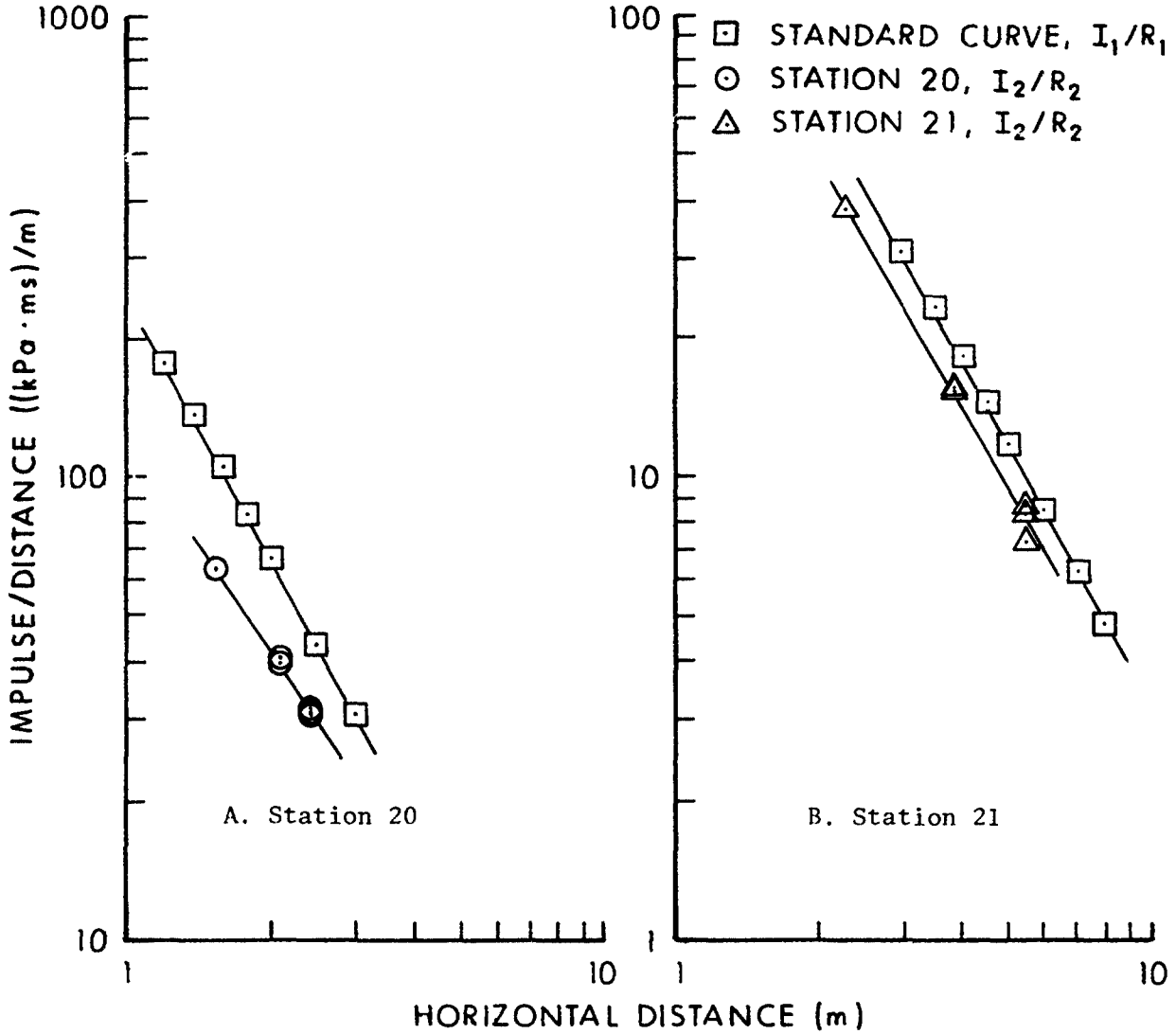

Figure 22. Comparison of Standard Free-Field Impulse to Data from Stations 20 and 21

TABLE 7. SUPPRESSION EFFECTS ON PRESSURE

Shot No.	Distance R_1 m	Distance R_2 m	Pressure kPa		TNT Equivalence kg
Station 20. Compared to Free Field Side-On Overpressure, Q_1 = 1 kg.					
1	2.00	1.52	279		0.44
2	2.90	2.20	125		0.44
3	2.70	2.20	143		0.54
4	3.35	2.43	93		0.38
5	3.30	2.43	95		0.40
6	3.45	2.43	86		0.35
				Avg.	0.43
Station 21. Compared to Free Field Side-On Overpressure, Q_1 = 1 kg.					
1	2.55	2.29	162		0.72
2	3.70	3.90	76		1.17
3	3.95	3.90	67		0.96
4	6.35	5.52	29		0.66
5	5.00	5.52	43		1.35
6	5.15	5.52	41		1.23
				Avg.	1.02
Calculated from Equation 2 Above - Analysis Section					
All	--	--	--		0.38

TABLE 8. SUPPRESSION EFFECTS ON IMPULSE

Shot No.	Experiment I_2 kPa-ms	Experiment R_2 m	Ratio I_2/R_2 kPa-ms/m	Standard I_1 kPa-ms	Standard R_1 m	Ratio I_1/R_1 kPa-ms/m	Ratio R_2/R_1	Q_2 $(R_2/R_1)^3$
			Station 20 Compared to Free-Field Side-On Impulse					
1	97	1.523	63.69	131	2.05	63.69	0.74	0.41
2	86	2.195	39.18	102	2.60	39.18	0.84	0.59
3	89	2.195	40.55	103	2.55	40.55	0.86	0.64
4	78	2.427	32.14	94	2.92	32.14	0.83	0.57
5	81	2.427	33.37	96	2.88	33.37	0.84	0.59
6	75	2.427	30.90	93	3.00	30.90	0.81	0.53
							Avg.	0.56
			Station 21 Compared to Free-Field Side-On Impulse					
1	88	2.286	38.50	103	2.675	38.50	0.86	0.64
2	61	3.902	15.63	67.7	4.33	15.63	0.90	0.73
3	60	3.902	15.38	67.0	4.35	15.38	0.90	0.73
4	40	5.519	7.25	47.1	6.50	7.25	0.85	0.61
5	48	5.519	8.70	50.9	5.85	8.70	0.94	0.83
6	46	5.519	8.33	50.4	6.05	8.33	0.91	0.75
							Avg.	0.72

B. Translation Velocity Predictions for Near Side-Wall

A listing of the pressure-time loading records obtained from the experiment showed that the near side-wall had the highest load values. The pressure-time records for Stations 1-6 on the near side-wall were weighted, according to wall location, and summed to obtain a total load. From this load an average pressure load was calculated for the entire near side-wall. Figure 23 shows the resulting pressure-time curves for each of the separation distances.

The digitized versions of these loads were used in a translation program which was run on a microcomputer. The assumption was made that the near-wall started to move when the pressure load was applied. This assumption was made because of the inherent structural weakness of the brick wall of the full-size magaziue which was modeled.

The computer program calculated the acceleration, a, from the model and loading parameters using Equation 4 for discrete intervals of the loading-time curve, P_L vs ti. Time intervals of 10-25 μs were used in the calculations.

$$a = 1000 \frac{A_W P_L}{M_W}, \tag{4}$$

where a is the acceleration (m/s^2) of the concrete model wall of area A_w (0.050 m^2) and mass M_W (0.953 kg) under a pressure loding of P_L measured in kPa. The incremental velocity, ΔV (m/s), was obtained from Equation 5 for an acceleration value over a time increment, Δt(s).

$$\Delta V = a \Delta t, \tag{5}$$

where the time increment, Δt, is from a time t_1 to t_2 and so on. The incremental distance ΔD(m), is found from Equation 6.

$$\Delta D = \frac{\Delta V}{2} \Delta t, \tag{6}$$

where ΔV and Δt are defined above. The factor of 1/2 is used to average the velocity changes over the time increment. The distance is then summed with each additional velocity and time increment.

The predicted motion parameters for the near-side wall are shown in Tables 9-11. The velocities are plotted in Figure 24. Generally, the velocity initially increases quickly, then reaches a maximum velocity at the end of the positive loading phase. Shot 2 had two major peaks in the pressure-time loading, which are seen in the wall velocity-time plot. When the second loading peak arrived, at 2 ms, the velocity sharply increased and reached a maximum above that of Shot 5 after it was lower initially. The maximum wall velocities reached ranged between 7-12 m/s.

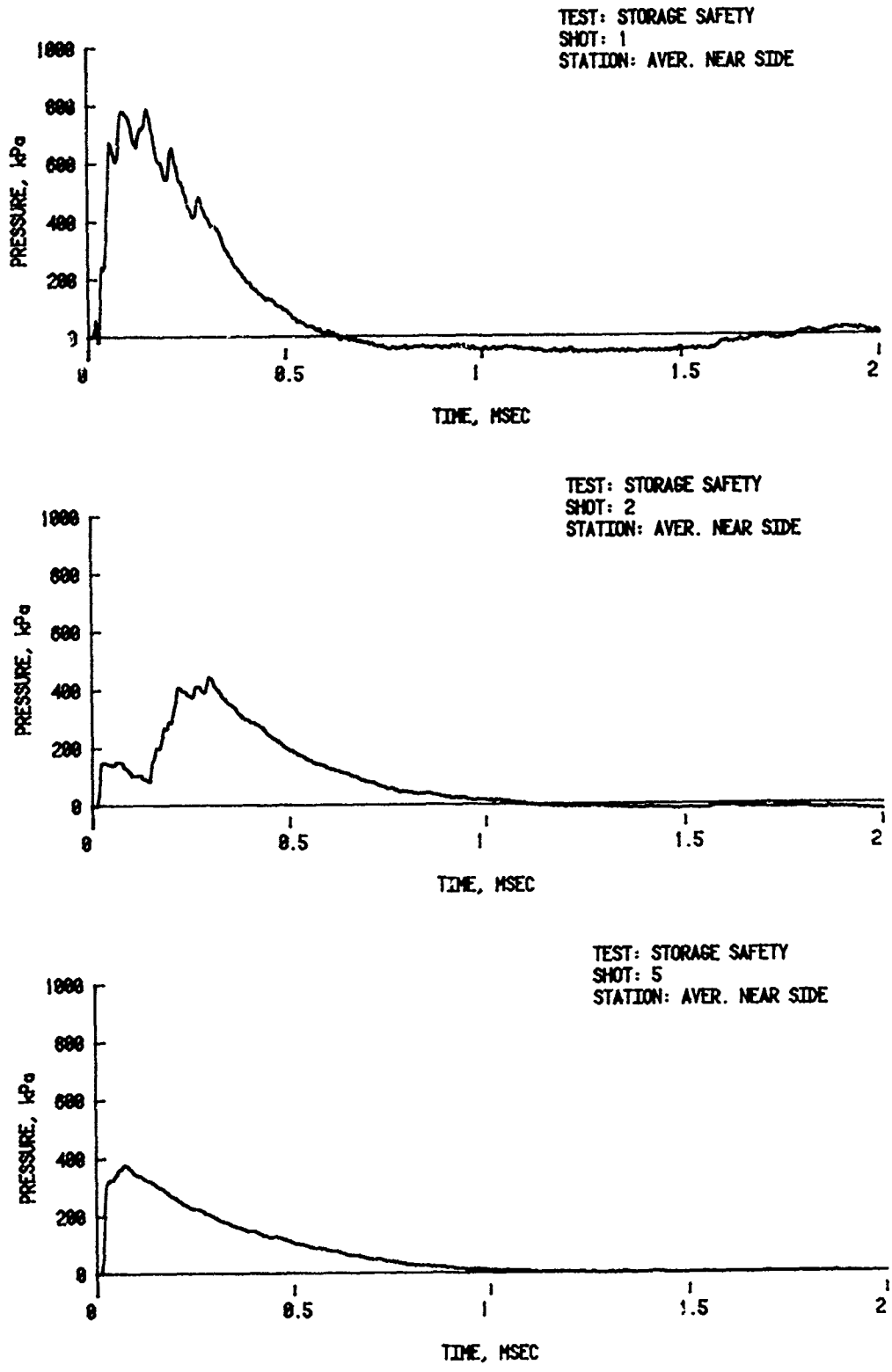

Figure 23. Average Loading on Near Side-Wall

Table 9. TRANSLATION OF NEAR SIDE-WALL,SHOT 1, 0.8 $Q^{1/3}_m$

Time, ms	Distance, cm	Velocity, m/s	Acceleration, m/s^2
0.00	0.00	0.00	0
0.03	0.01	0.71	35930
0.06	0.02	1.73	35930
0.10	0.03	3.32	36350
0.15	0.04	5.28	40350
0.19	0.06	6.61	29210
0.25	0.11	8.40	24790
0.30	0.15	9.57	22020
0.35	0.20	10.46	14390
0.40	0.25	11.02	9910
0.45	0.35	11.38	5600
0.50	0.36	11.57	2670
0.55	0.42	11.63	800
0.58	0.45	11.64	107

Table 10. TRANSLATION OF NEAR SIDE-WALL, SHOT 2, 1.6 $Q^{1/3}$

Time, ms	Distance, cm	Velocity, m/s	Acceleration, m/s^2
0.00	0.00	0.00	0
0.03	0.00	0.19	7730
0.08	0.00	0.58	8000
0.10	0.01	0.74	6400
0.15	0.02	0.93	9530
0.19	0.03	1.36	15030
0.25	0.04	2.76	21590
0.29	0.05	3.27	19990
0.35	0.06	4.94	23450
0.45	0.10	6.84	15780
0.55	0.19	8.13	10450
0.65	0.27	8.96	7090
0.75	0.37	9.51	4420
0.85	0.47	9.83	2560
0.95	0.55	10.03	1870
1.08	0.65	10.16	910
1.12	0.75	10.19	267

Table 11. TRANSLATION OF NEAR SIDE-WALL, SHOT 5, 2.4 $Q^{1/3}$ m

Time,ms	Distance,cm	Velocity, m/s	Acceleration, m/s^2
0.00	0.00	0.00	0
0.03	0.01	0.43	17060
0.08	0.02	1.38	20040
0.15	0.03	2.69	16470
0.20	0.04	3.43	14130
0.25	0.05	4.05	11990
0.30	0.07	4.60	10390
0.35	0.10	5.06	8850
0.40	0.12	5.45	7680
0.45	0.15	5.79	6660
0.50	0.17	6.09	5700
0.55	0.02	6.34	4690
0.60	0.22	6.53	3739
0.65	0.28	6.69	3200
0.70	0.30	6.82	2400
0.75	0.33	6.92	1870
0.85	0.42	7.06	1170
0.95	0.50	7.13	590
1.05	0.55	7.18	320
1.15	0.70	7.21	107
1.25	0.75	7.22	80
1.35	0.80	7.22	53

None of these maximum velocities appears great enough to initiate candidate munitions (Reference 1) that may be stored in this type of above ground, barricaded storage magazine.

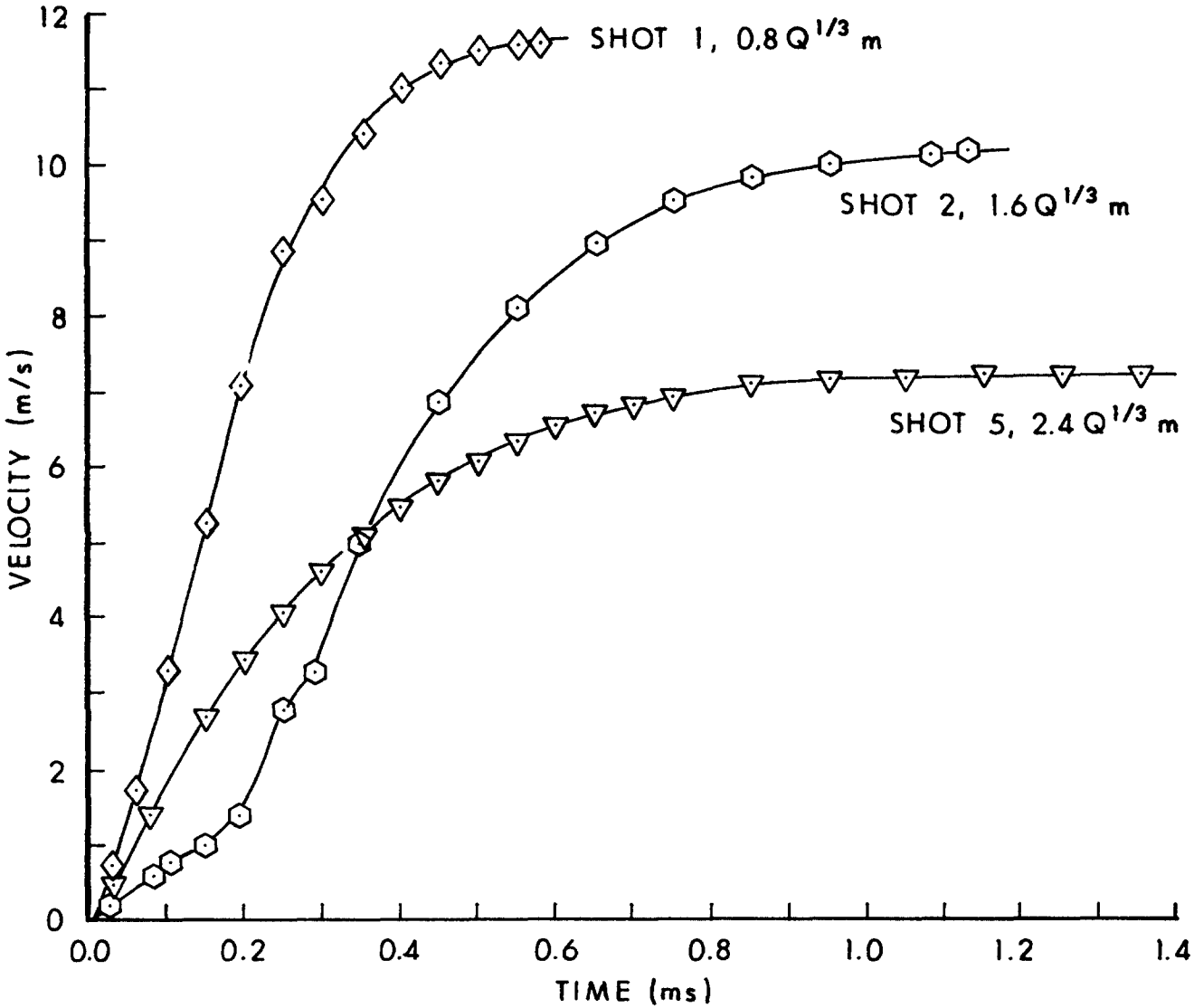

Figure 24. Predicted Translational Velocity of Near Side-Wall

SUMMARY AND CONCLUSIONS

A test series of six shots was fired with 1 kg bare 50/50 Pentolite hemispherical charges placed inside model concrete donor magazines. Measurements of pressure-time loading were obtained at several locations on a nonresponding barricaded model acceptor magazine. The experimental models were constructed at 1/23.5 scale of the full sized above ground barricaded munition storage magazine on site at Machrihanish, Scotland.

Calculations of charge suppression factors for Station 20 (using a pressure method), caused by the cover of the concrete donor model over the base charge, indicate values around 0.43 kg. A 0.43 kg free-field base hemispherical charge would have pressure equivalency to the covered 1 kg charge used during the experiments. At the greater distances, as calculated for Station 21, the average charge suppression factor was 1.02 kg indicating little or no effect of the donor model cover, or of the barricades around the model.

Whole wall translation velocities, calculated from the average near side-wall loading, ranged from 7-12 m/s. These low predicted velocities seem to be born out from the results of a preliminary shot with a responding concrete acceptor model magazine. Component wall debris translation appeared to be minimal. Tentatively, the observed and calculated values for the near side-wall (the highest loaded surface) velocities, indicated that the components of the wall would not attain hazardous velocities as quoted in the literature. This was true at a standard safe separation distance of $0.8\ Q^{1/3}$ m. It would appear not necessary to increase the separation distance from this value to any larger separation distance. The $0.8\ Q^{1/3}$ m separation distance appears adequate.

Further experiments are planned to better determine the velocities of wall debris from a number of responding model acceptor walls. Time constraints of the present experiments allowed only preliminary debris results to be obtained.

ACKNOWLEDGMENT

The authors wish to thank Mr. Kenneth Holbrook for the very extensive site and model preparation and also for being the explosive handler for the test series.

REFERENCES

1. F. B. Porzel and J. M. Ward, "Explosive Safety Analysis of the Machrianish Magazine," NSWC TR 79-359, December 1979.

2. Charles N. Kingery, Gerald Bulmash, and Peter C. Muller, "Blast Loading on Above Ground Barricaded Munition Storage Magazines," Ballistic Research Laboratory Technical Report ARBRL-TR-0257, May 1984 (A141677).

3. "Structures to Resist the Effects of Accidental Explosions," Dept. of the Army Technical Manual TM 5-1300, June 1969.

4. Private Communication from Mr. Gerald Bulmash, USA Ballistic Research Laboratory, Aberdeen Proving Ground, MD 21005-5066.

5. Wilfred E. Baker, Explosions in Air, University of Texas Press, Austin, TX, 1973.